EBioMedicine 2 (2015) 1767–1784

Contents lists available at ScienceDirect

EBioMedicine

journal homepage: www.ebiomedicine.com

Research Article

Cyclic AMP Response Element Binding Protein Mediates Pathological Retinal Neovascularization via Modulating DLL4-NOTCH1 Signaling

Nikhlesh K. Singh, Sivareddy Kotla, Raj Kumar, Gadiparthi N. Rao *

Department of Physiology, University of Tennessee Health Science Center, Memphis, TN 38163, USA

ARTICLE INFO

Article history:
Received 17 April 2015
Received in revised form 8 September 2015
Accepted 23 September 2015
Available online 28 September 2015

Keywords:
CREB
DLL4
NOTCH1
VEGFC
Retinal neovascularization

ABSTRACT

Retinal neovascularization is the most common cause of moderate to severe vision loss in all age groups. Despite the use of anti-VEGFA therapies, this complication continues to cause blindness, suggesting a role for additional molecules in retinal neovascularization. Besides VEGFA and VEGFB, hypoxia induced VEGFC expression robustly. Based on this finding, we tested the role of VEGFC in pathological retinal angiogenesis. VEGFC induced proliferation, migration, sprouting and tube formation of human retinal microvascular endothelial cells (HRMVECs) and these responses require CREB-mediated DLL4 expression and NOTCH1 activation. Furthermore, down regulation of VEGFC levels substantially reduced tip cell formation and retinal neovascularization in vivo. In addition, we observed that CREB via modulating the DLL4-NOTCH1 signaling mediates VEGFC-induced tip cell formation and retinal neovascularization. In regard to upstream mechanism, we found that down regulation of p38β levels inhibited hypoxia-induced CREB-DLL4-NOTCH1 activation, tip cell formation, sprouting and retinal neovascularization. Based on these findings, it may be suggested that VEGFC besides its role in the regulation of lymphangiogenesis also plays a role in pathological retinal angiogenesis and this effect depends on p38β and CREB-mediated activation of DLL4-NOTCH1 signaling.

1. Introduction

Retinal neovascularization is the most common cause of moderate to severe vision loss in all age groups; i.e., retinopathy of prematurity (ROP) in children, diabetic retinopathy in adults and age-related macular degeneration in the elderly (Andreoli and Miller, 2007; Chen and Smith, 2007; Ferrara and Kerbel, 2005). These various retinal neovascular pathologies, in turn, may cause vitreous hemorrhage, retinal detachment and/or neovascular glaucoma affecting vision (Aiello et al., 1994). A large body of evidence shows that vascular endothelial growth factor A (VEGFA) is one of the major factors linked to the pathogenesis of proliferative retinopathy (Alon et al., 1995). The VEGF family consists of 7 structurally related molecules (VEGF-A through F and placental growth factor) that bind to 3 tyrosine kinase receptors (VEGFR1, 2 and 3) with different affinities (Karkkainen and Petrova, 2000). VEGFA has been the focus of many current anti-angiogenesis regimens as it was the most characterized angiogenic and permeability factor implicated in various pathologies including retinal neovascularization (Kuiper et al., 2008). However, the anti-VEGFA therapies have been observed to have some deleterious effects such as an increase in the expression of connective tissue growth factor (CTGF), which promotes a switch from angiogenesis to fibrosis (Kuiper et al., 2008). In addition, 82% of the tractional retinal detachments (TRDs) were reported linked to anti-VEGFA injections (Arevalo et al., 2008). Furthermore, besides VEGFA, other molecules such as VEGFC and VEGFD have been reported to play a role in angiogenesis and lymphangiogenesis via activation of VEGFR2 and VEGFR3 (Achen et al., 1998; Cao et al., 1998). Although, the initial studies have reported that the expression of VEGFR3 is restricted to lymphatic endothelium (Jeltsch et al., 1997; Kaipainen et al., 1995), it is now recognized that the VEGFC–VEGFR3 signaling also modulates the branching morphogenesis of blood vessels (Tammela et al., 2008). Despite these advances in our understanding of the role of VEGFC in angiogenesis and lymphangiogenesis, its involvement in pathological retinal angiogenesis is not explored.

The cyclic adenosine monophosphate (cAMP)-response element-binding protein (CREB) is a transcription factor that belongs to the basic leucine-zipper family and binds to a specific regulatory element known as cAMP-response element (CREs) in the promoters of its target genes and enhances their expression (Shaywitz and Greenberg, 1999). CREB mediates hypoxia-induced expression of a number of genes, including VEGFA and its receptors (Kang et al., 2014; Leonard et al., 2008; Morishita et al., 1995; Wu et al., 2007). Many studies have also demonstrated that VEGFA, FGF2 and hepatocyte growth factor by phosphorylating increase CREB transcriptional transactivation activity in endothelial cells (Abramovitch et al., 2004; Hoot et al., 2010; Kottakis et al., 2011; Zhao et al., 2011). Furthermore, it has been

* Corresponding author at: Department of Physiology, University of Tennessee Health Science Center, 894 Union Avenue, Memphis, TN 38163, USA.
E-mail address: rgadipar@uthsc.edu (G.N. Rao).

http://dx.doi.org/10.1016/j.ebiom.2015.09.042

reported that overexpression of constitutively active CREB aggravates tumor angiogenesis (Abramovitch et al., 2004). Despite these clues linking CREB to the modulation of angiogenesis, its developmental or pathological angiogenesis is not known. In the present study, we used a mouse model of retinopathy to understand the role of CREB in pathological retinal neovascularization. The mouse model of retinopathy which involves an initial phase of hyperoxia-induced vessel loss, followed by a phase of hypoxia-induced pathological neovascularization (Smith et al., 1994), allowed us to decipher the role of VEGFC and CREB axis in pathological retinal neovascularization. Our results for the first time demonstrate that CREB by modulating DLL4–NOTCH1 signaling plays a crucial role in pathological retinal angiogenesis.

2. Materials and Methods

2.1. Reagents

Growth factor-reduced Matrigel (354,230) was obtained from BD Biosciences (Bedford, MA). Recombinant human VEGFB167 (751-VE), recombinant human VEGFC (2179-VC), recombinant human VEGFD (622-VD) and anti-VEGFR3 (AF743) antibodies were bought from R & D Systems (Minneapolis, MN). Anti-GFP (SC-9996), anti-JNK1/3 (SC-474), anti-β-tubulin (SC-9104), anti-VEGFA (SC-152), anti-VEGFB (SC-80,442), anti-VEGFC (SC-130,289) and anti-VEGFD (SC-13,085) antibodies were purchased from Santa Cruz Biotechnology (Santa Cruz, CA). Anti-pCREB (9198), anti-CREB (4820), anti-pJNK1 (9251) and anti-pp38MAPK (9198) antibodies were obtained from Cell Signaling Technology (Beverly, MA). Anti-NOTCH2 (07–1234) antibodies were bought from Millipore (Temecula, CA). Anti-CD31 (550,274) antibody was purchased from BD Pharmingen (Palo Alto, CA). Anti-DLL1 (ab84620), anti-DLL4 (ab7280), anti-Ki67 (ab15580), anti-NOTCH1 (ab52627) and anti-NOTCH4 (ab166605) antibodies were obtained from Abcam (Cambridge, MA). Anti-NOTCH1 antibody (NB100-78,486) was bought from Novus Biologicals (Littleton, CO). Thirty μ-Dish 35 mm, low culture-inserts were purchased from ibidi (Munich, Germany). EGM2 medium was purchased from Lonza (Basel, Switzerland). Control nontargeting small interfering RNA (siRNA) (D-001,810-10), human DLL4 siRNA (ON-TARGET plus SMARTpool L-010,490-00), human NOTCH1 siRNA (ON-TARGET plus SMARTpool L-007,771-00), mouse CREB siRNA (ON-TARGET plus SMARTpool L-040,591-00), mouse DLL4 siRNA (ON-TARGET plus SMARTpool L-045,947-00), mouse JNK1 siRNA (ON-TARGET plus SMARTpool L-040,128-00), mouse p38MAPKβ siRNA (ON-TARGET plus SMARTpool L-040,613-00), mouse NOTCH1 siRNA (ON-TARGET plus SMARTpool L-041,110-00), mouse VEGFC siRNA (ON-TARGET plus SMARTpool L-012,071-00) and anti-p38MAPKβ (PA5-14,425) antibodies were obtained from Thermo Scientific (Chicago, IL). Cell Tracker Green (C7025), Alexa Fluor 488-conjugated goat anti-rat immunoglobulin G, Alexa Fluor 568-conjugated goat anti-rabbit immunoglobulin G, Hoechst 33,342, isolectin B4-594, and Prolong Gold antifade reagent were bought from Molecular Probes (Eugene, OR). Cytodex beads (C3275) and thrombin (T8885) were purchased from SIGMA-ALDRICH (St. Louis, MO). Bovine fibrinogen (820,224) was purchased from MP Biomedicals (Irvine, CA). [^{3}H]-Thymidine (S. A. 20 Ci/mM) was obtained from Perkin Elmer (Boston, MA).

2.2. Generation of Conditional Knockout Mice

To delete CREB in the postnatal vasculature, we interbred CREB$^{flox/flox}$ mice (Mantamadiotis et al., 2002) with transgenic mice expressing the tamoxifen-inducible recombinase (CreERT2) under the control of the endothelial Cdh5 promoter (Wang et al., 2010). CREB$^{flox/-}$:Cdh5-CreERT2 mice were interbred with CREB$^{flox/flox}$ to generate CREB$^{flox/flox}$:Cdh5-CreERT2 litters. To induce Cre activity and gene deletion, two consecutive intraperitoneal tamoxifen (Sigma-Aldrich, T5648; 2 mg/ml; generated by dissolving in 10% ethanol and 90% corn oil) injections of 50 μl were given at P10 and P11 to generate endothelial specific deletion of CREB (CREB$^{i\Delta EC}$). The Animal Care and Use Committee of the University of Tennessee Health Science Center, Memphis, TN, approved all the experiments involving the use of animals.

2.3. Cell Culture

HRMVECs (ACBRI 181) were purchased from Applied Cell Biology Research Institute (Kirkland, WA) and grown in medium 131 containing microvascular growth supplements (MVGS), 10 μg/ml gentamycin, and 0.25 μg/ml amphotericin B. Cultures were maintained at 37°C in a humidified 95% air and 5% CO_2 atmosphere. HRMVECs with passage numbers between 5 and 10 were synchronized by incubating in medium 131 without MVGS for 24 h and used to perform the experiments unless otherwise indicated.

2.4. Cell Migration

Cell migration was measured by wounding assay as described by us previously (Singh et al., 2015). Briefly, HRMVECs were plated at 2×10^5 cells/ml in each chamber of the ibidi culture-inserts, grown to full confluency and growth-arrested. Following a 12-h growth-arresting period, the inserts were removed using sterile tweezers and 1 ml of medium 131 containing 5 mM hydroxyurea was added to the culture dish. Cells were treated with and without VEGFC (100 ng/ml) for 24 h and cell migration was observed under Nikon Eclipse TS100 microscope with 10×/0.25 magnification and the images were captured with a CCD color camera (KP-D20AU; Hitachi, Ibaraki, Japan) using Apple iMovie 7.1.4 software. The cell migration was expressed as percent wound closure (total wound area at 0 h minus wound area at 24 h/total wound area at 0 h × 100).

2.5. DNA Synthesis

DNA synthesis was measured by [^{3}H]-thymidine incorporation using 3D ON-TOP assay (Lee et al., 2007). Briefly, quiesced HRMVECs were trypsinized to a single-cell suspension and 1×10^5 cells in 0.5 ml of the medium were plated onto a matrigel-coated surface of a 24-well plate and VEGFC (100 ng/ml) or vehicle were added to the medium. Cells were allowed to settle for 30 min at 37°C, following which 0.5 ml of medium containing 10% matrigel was added on top of the cells. Six hours later, the cells were pulse-labeled with 1 μCi/ml of [^{3}H]-thymidine for 24 h, at which time cells were washed with cold PBS, collected along with matrigel in 3 ml of 5 mM EDTA in cold PBS into 15 ml centrifuge tubes. The tubes were kept on ice for 15 min to allow the breakdown of matrigel. The cells were then added with 3 ml of 20% (*w*/*v*) cold TCA and vortexed vigorously to lyse the cells. The cell mixture was allowed to remain on ice for 30 min and then passed through a GF/F glass microfiber filter. The filter was washed once with 5% cold TCA and once with cold ethanol, dried, placed in a liquid scintillation vial containing the scintillation fluid and the radioactivity was measured in a liquid scintillation counter (Beckman LS 3801). DNA synthesis was expressed as counts/min/well.

2.6. Sprouting Assay

Three-dimensional sprouting was performed according to a previously described protocol (Nakatsu and Hughes, 2008). Briefly, the HRMVECs transfected with the indicated siRNA or transduced with the indicated adenovirus were coated on Cytodex beads and allowed to attach overnight. The beads were embedded in fibrin gels and fibroblasts were added onto the top of the gels. Sprouting was examined on day 3 under Zeiss inverted fluorescence microscope (Carl Zeiss AxioVision Observer.Z1; original magnification × 10/NA 0.45) and the fluorescence images were captured using Zeiss AxioCam MRm camera and the microscope operating and image analysis software AxioVision 4.7.2

(Carl Zeiss Imaging Solutions GmbH). Sprouting was expressed as number of sprouts/bead.

2.7. Tube Formation

Tube formation was measured as described previously (Singh et al., 2013). Quiescent HRMVECs were placed in 24-well culture dishes (Costar; Corning) coated with growth factor-reduced Matrigel (BD Biosciences). Vehicle or VEGFC were added and the cells were incubated at 37°C for 6 h. When siRNA or adenoviral vectors were used, cells were transfected with the indicated siRNA or transduced with the indicated adenovirus and quiesced before they were subjected to tube formation assay. After 6 h of incubation, tube formation was observed under an inverted microscope (Eclipse TS100; Nikon, Tokyo, Japan) and the images were captured with a CCD color camera (KP-D20AU; Hitachi, Ibaraki, Japan) using Apple iMovie 7.1.4 software. The tube length was calculated using NIH ImageJ version 1.43 and expressed in micrometers.

2.8. Western Blotting

Cell or tissue extracts containing an equal amount of protein were resolved by electrophoresis on 0.1% (weight/volume [*w*/*v*]) sodium dodecyl sulfate and 10% (*w*/*v*) polyacrylamide gels. The proteins were transferred electrophoretically to a nitrocellulose membrane. After blocking in either 5% (*w*/*v*) nonfat dry milk or bovine serum albumin, the membrane was probed with the appropriate primary antibodies followed by incubation with horseradish-peroxidase-conjugated secondary antibodies. The antigen-antibody complexes were detected using an enhanced chemiluminescence detection reagent kit (Amersham Biosciences).

2.9. Transfections

HRMVECs were transfected with control or target siRNA molecules at a final concentration of 100 nM using Lipofectamine 2000 transfection reagent according to the manufacturer's instructions. After transfections, cells were growth-arrested in MVGS-free medium 131 for 24 h and used as required.

2.10. Oxygen-Induced Retinopathy (OIR)

OIR was performed as described by Smith et al. (1994) and quantified according to the method of Connor et al. (2009). C57BL/6 mice pups (P7) with dams were exposed to 75% oxygen for 5 days and then returned to room air at P12. Mice pups of the same age kept at room air were used as controls. Mice pups were sacrificed at P17 and eyes were enucleated and fixed in 4% (*v*/*v*) paraformaldehyde for 1 h at room temperature. Retinas were isolated, stained with isolectin B4, flat mounted, placed under a coverslip, and examined by a Zeiss inverted fluorescence microscope (Axio Observer.Z1). Retinal vasculature was quantified by calculating the ratio of fluorescence intensity to total retinal area. Retinal neovascularization was quantified by first setting a scale with a tolerance point of 50 based on the fluorescence intensity in the screenshot using Nikon NIS-Elements software version AR 3.1. Neovascularity was highlighted in red and then quantified by dividing the fluorescence intensity in the highlighted area by the total fluorescence intensity in the screenshot (n = 6 eyes).

2.11. Intravitreal Injections

After exposure to hyperoxia, pups were administered with scrambled, or the indicated siRNA at 1 μg/0.5 μl/eye) by intravitreal injections using a 33G needle.

2.12. Immunofluorescence Staining

After hyperoxia, mouse pups were returned to room air for 3 days, after which time they were sacrificed, eyes enucleated and fixed in optimal cutting temperature compound, and 8-μm cryosections were prepared from the central part of the retina. To identify proliferating ECs, after blocking in normal goat serum, the cryosections were probed with rabbit anti-mouse Ki67 antibodies (1:100) and rat anti-mouse CD31 antibodies (1:100) followed by incubation with Alexa Fluor 568-conjugated goat anti-rabbit and Alexa Fluor 488-conjugated goat anti-rat secondary antibodies. The sections were observed under Zeiss inverted microscope (Axio Observer.Z1; type, LD plan-Neofluar; original magnification X40/NA 0.6 or type, plan-Apochromat; original magnification X10/NA 0.45) and the fluorescence images were captured by Zeiss AxioCam MRm camera using the microscope operating and image analysis software AxioVision 4.7.2 (Carl Zeiss Imaging Solutions GmbH). The retinal EC proliferation was quantified by counting Ki67- and CD31-positive cells that extended anterior to the inner limiting membrane per section (n = 6 eyes, 3 sections/eye).

2.13. DLL4 Promoter Cloning

Using HRMVEC genomic DNA as a template, DLL4 promoter fragment from −2210 nucleotides (nt) to +78 nt was amplified by polymerase chain reaction using a forward primer, 5′-GAGCTCCTGCCCGGTTGGACTGGGGA-3′ incorporating a SacI restriction enzyme site at the 5′-end and a reverse primer, 5′- AGATCTACGGAGTCTTGCTCTGTCACTCA-3′ incorporating BglII restriction site at the 5′-end. The resulting ~2.2 kb PCR product was digested with SacI and BglII and cloned into SacI and BglII sites of the pGL3 basic vector (Promega) to yield pGL3-hDLL4 (2.2 kb). To generate 5′-truncated promoter fragment starting from −605 nt, forward primer, 5′-GAGCTCACCTGGTTCCTGCTCATTCTCTTCC-3′, and reverse primer, hDLL4-R, 5′-AGATCTACGGAGTCTTGCTCTGTCACTCA-3′, were used in the PCR. The PCR products were digested with SacI and BglII and cloned into SacI and BglIII sites of the pGL3 basic vector to yield pGL3-hDLL4 (0.68 kb). The underlined regions are SacI and BglII sites in both the forward and the reverse primers, respectively. Site-directed mutations within the CREB-binding element at −193 nt were introduced by using the QuickChange site-directed mutagenesis kit according to manufacturer's instructions and using the following primers: forward, 5′-GTGAGTTTCCCTGGCAGGACC*TC*CGTCAGTTCCAGTTGTGTTG-3′ and reverse, 5′-CAACACAACTGGAACTGACGGAGGTCCTGCCAGGGAAACTCAC-3′ to yield pGL3-hDLL4m. The boldface letters indicate the mutated bases. Clones were verified by DNA sequencing using pGL3 vector-specific primers.

2.14. Luciferase Assay

HRMVECs cells were transfected with pGL3 empty vector or pGL3-hDLL4 (2.2 kb and 0.68 kb) promoter constructs with and without the indicated mutations using Lipofectamine 2000 transfection reagent. After growth arrest in serum-free medium for 12 h, cells were treated with and without VEGFC (100 ng/ml) for 4 h, washed with cold PBS, and lysed in 200 μl of lysis buffer. The cell extracts were cleared by centrifugation at 12,000 rpm for 2 min at 4°C. The supernatants were assayed for luciferase activity using a luciferase assay system (Promega) and a single tube luminometer (TD20/20; Turner Designs, Sunnyvale, CA) and expressed as relative luciferase units.

2.15. Chromatin Immunprecipitation (ChIP) Assay

ChIP assay was performed on HRMVECs with and without the indicated treatments using a kit and following the supplier′s protocol (Upstate Biotechnology Inc., Lake Placid, NY). CREB–DNA complexes were immunoprecipitated using anti-CREB antibodies. Preimmune mouse serum was used as a negative control. The immunoprecipitated

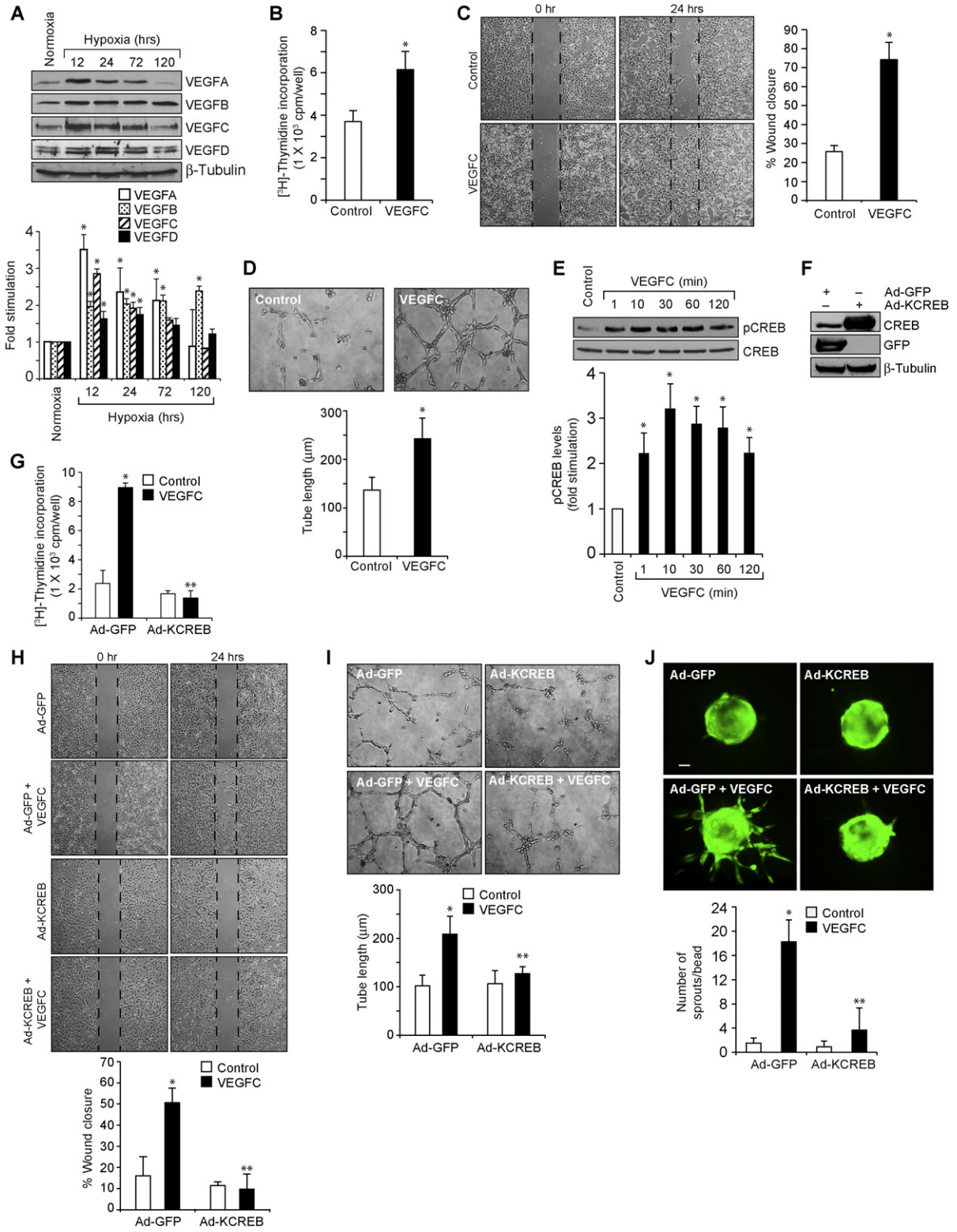

Fig. 1. CREB mediates VEGFC-induced angiogenic events. A. C57BL/6 mice pups after exposure to 75% oxygen from P7 to P12 were returned to room air to develop the relative hypoxia. Eyes from pups left in normoxia or at various time periods of hypoxia were enucleated, retinas isolated and extracts were prepared. An equal amount of protein from normoxic and various time periods of hypoxic retinal extracts was analyzed by Western blotting for VEGFA, VEGFB, VEGFC and VEGFD levels using their specific antibodies and normalized to β-tubulin. B–D. Quiescent HRMVECs were treated with and without VEGFC (100 ng/ml) and DNA synthesis (B), migration (C), or tube formation (D) were measured. E. An equal amount of protein from control and the indicated time periods of VEGFC (100 ng/ml)-treated HRMVECs was analyzed by Western blotting for pCREB levels using its phospho-specific antibodies and normalized to CREB. F. Cells were transduced with Ad-GFP or Ad-KCREB (40 moi) and 48 h later cell extracts were prepared and analyzed for over expression of GFP or KCREB by Western blotting using their specific antibodies and normalized to β-tubulin. G–I. All the conditions were the same as in panel F except that after transduction with the adenovirus, cells were quiesced and subjected to VEGFC (100 ng/ml)-induced DNA synthesis (G), migration (H), or tube formation (I). J. All the conditions were the same as in panel F except that after transduction, cells were labeled with Cell Tracker Green, coated onto Cytodex beads, embedded in a 3D-fibrin gel in EGM2 medium for 3 days and sprouts were observed under fluorescent microscope. The images were captured using MRm camera. The bar graphs represent quantitative analysis of three independent experiments. The values are presented as Mean ± SD. * $p < 0.01$ vs control, normoxia or Ad-GFP; ** $p < 0.01$ vs Ad-GFP + VEGFC. Scale bar represents 50 μm.

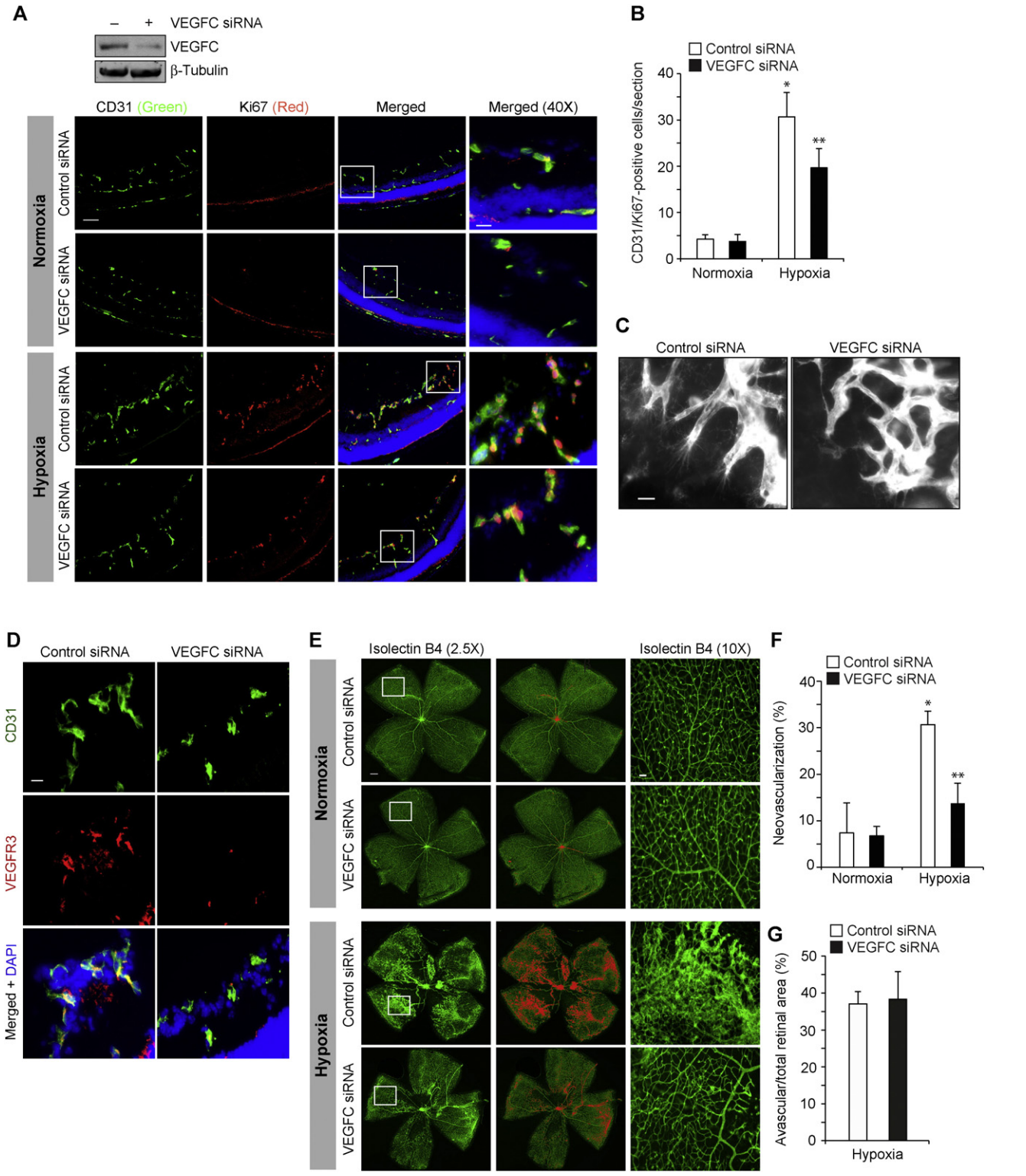

Fig. 2. VEGFC mediates hypoxia-induced retinal neovascularization. A. After exposure to 75% oxygen from P7 to P12, pups were returned to room air to develop the relative hypoxia. Pups were administered intravitreally with 1 μg/0.5 μl/eye of control or VEGFC siRNA at P12 and P13 and at P15 the retinas were isolated and either tissue extracts were prepared and analyzed for VEGFC levels by Western blotting using its specific antibody and normalized to β-tubulin or fixed, cross-sections made and stained by immunofluorescence for CD31 and Ki67. The right column shows the higher magnification (40×) of the areas selected by rectangular boxes in the left column images. B. Retinal EC proliferation was measured by counting CD31- and Ki67-positive cells that extended anterior to the inner limiting membrane per section (n = 6 eyes, 3 sections/eye). C. All the conditions were the same as in panel A except that control or VEGFC siRNAs were injected intravitreally at P12, P13, and P15 and at P17 the retinas were isolated, stained with isolectin B4, flat mounts were made and examined for EC filopodia formation at 40× magnification. D. All the conditions were the same as in panel A except that the sections were stained for CD31, VEGFR3 and DAPI. E. All the conditions were the same as in panel C except that retinal neovascularization was measured at 2.5× magnification. Retinal vascularization is shown in the first column. Neovascularization is highlighted in red in the second column. The third row shows the selected rectangular areas of the images in the first column under 10× magnification. F & G. Retinal neovascularization (F) and avascular area (G) were determined as described in "Materials and Methods." The bar graphs represent quantitative analysis of three blots or 6 retinas. The values are presented as Mean ± SD. * $p < 0.01$ vs normoxia + control siRNA; ** $p < 0.01$ vs hypoxia + control siRNA. Scale bar represents 50 μm and 20 μm in panel A, far left column and far right column, respectively, 20 μm in panels C & D, 300 μm and 50 μm in panel E, far left column and far right column, respectively.

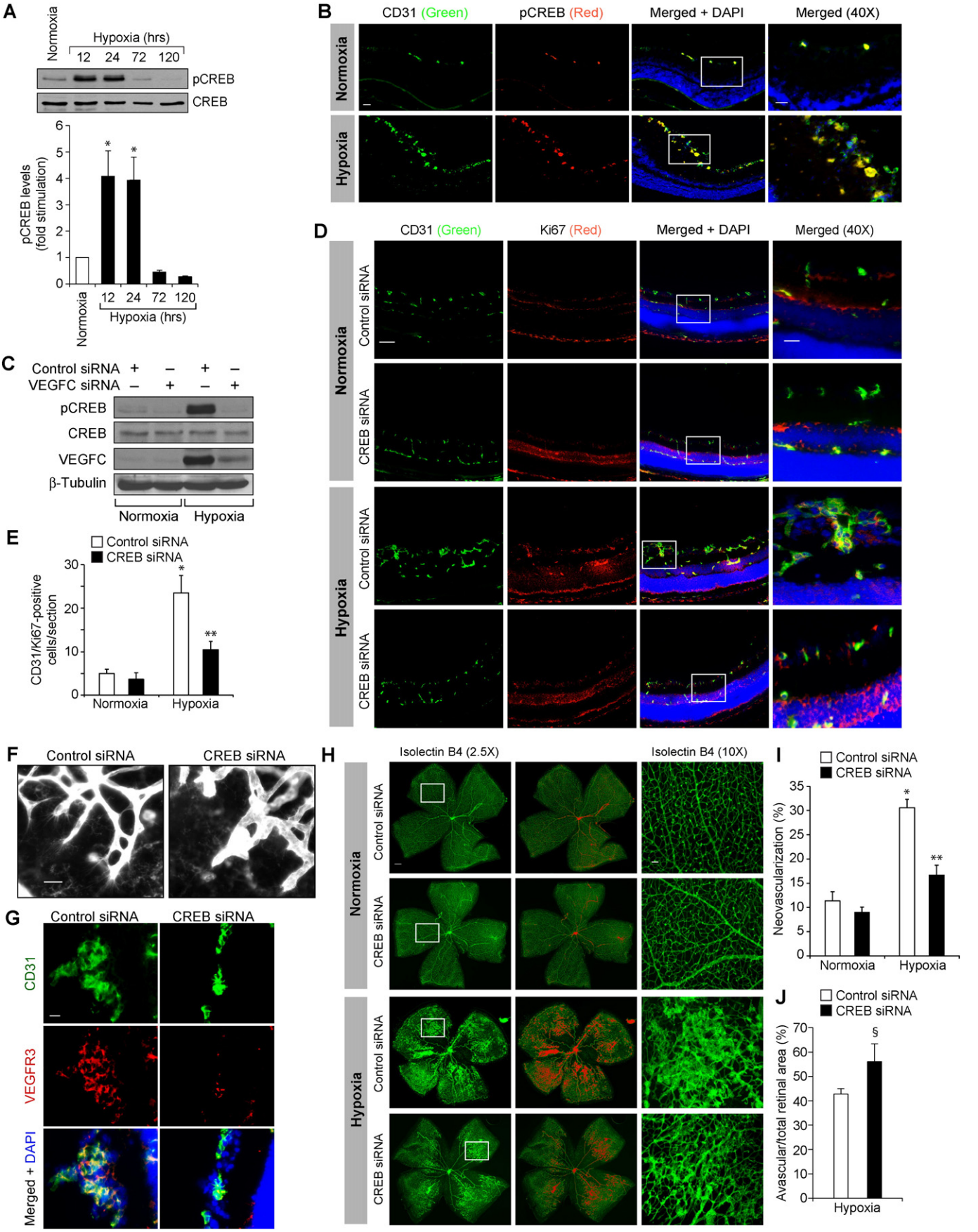
A
Normoxia
Hypoxia (hrs)
12 24 72 120
pCREB
CREB
pCREB levels (fold stimulation)
Normoxia
12 24 72 120
Hypoxia (hrs)
B
CD31 (Green)
pCREB (Red)
Merged + DAPI
Merged (40X)
Normoxia
Hypoxia
C
Control siRNA + – + –
VEGFC siRNA – + – +
pCREB
CREB
VEGFC
β-Tubulin
Normoxia
Hypoxia
D
CD31 (Green)
Ki67 (Red)
Merged + DAPI
Merged (40X)
Normoxia
Hypoxia
Control siRNA
CREB siRNA
E
Control siRNA
CREB siRNA
CD31/Ki67-positive cells/section
Normoxia
Hypoxia
F
Control siRNA
CREB siRNA
G
Control siRNA
CREB siRNA
CD31
VEGFR3
Merged + DAPI
H
Isolectin B4 (2.5X)
Isolectin B4 (10X)
Normoxia
Hypoxia
Control siRNA
CREB siRNA
I
Control siRNA
CREB siRNA
Neovascularization (%)
Normoxia
Hypoxia
J
Control siRNA
CREB siRNA
Avascular/total retinal area (%)
Hypoxia

DNA was uncross-linked, subjected to Proteinase K digestion, purified using QIAquick columns (Cat. No. 28,104, Qiagen, Valenica, CA), and used as a template for PCR amplification with primers, forward, 5′-CCATTTCTACCTGTTGAAAT-3′, and reverse, 5′- ATGACCAGTGCAGT CAACCA-3,′ that would amplify a 220 bp fragment encompassing the CREB-binding site at −193 nt and used as a template for PCR amplification with primers, forward, 5′-TTCCTTATCTTCATCCTA-3′, and reverse, 5′- ATGACCAGTGCAGTCAACCA-3 that would amplify 106 bp fragment encompassing the CREB binding site at −193 nt. The resulting PCR products were resolved on 1.8% agarose gels and stained with ethidium bromide and the images were captured using a Kodak In Vivo Imaging System. For quantification, the ChiP DNA was also subjected to qPCR using the same primers on 7300 Real-Time PCR Systems (Applied Biosystems) using SYBR Green PCR Master Mix (Cat. No. 4,309,155, Applied Biosystems) with the following conditions: 95°C for 10 min followed by 40 cycles at 95°C for 15 s with extension at 60°C for 1 min. Both IgG and anti-CREB–DNA Ct values were normalized to input DNA Ct values to obtain ΔCt values. Then ΔΔCt values were calculated by subtracting the ΔCt values of negative controls from the experimental ΔCt values. The fold enrichment of CREB-bound DLL4 promoter is calculated by using $2^{(-\Delta\Delta Ct)}$.

2.16. Electrophoretic Mobility Shift Assay

Nuclear extracts of HRMVECs with and without appropriate treatments were prepared as described previously (Potula et al., 2009). The protein content of the nuclear extracts was determined using a micro-BCA method. Biotin-labeled double-stranded oligonucleotides encompassing CREB-binding element at −193 nt (5′- TCCCTGGC AGGACTGACGTCAGTTCCAG-3′) and its complementary sequence was used as a probe. Briefly, 5 μg of nuclear extract was incubated in a binding buffer with 2.5 nmole biotin-labeled probe and 2 μg poly dI:dC for 30 min at room temperature in 20 μl binding reaction buffer (10 mM Tris–HCl, pH 7.9, 50 mM KCl, 1 mM DTT, 15% glycerol). The DNA-protein complexes were analyzed by electrophoresis on 6% polyacrylamide gel and visualized by chemiluminescence. To perform a supershift electrophoretic mobility shift assay, the complete reaction mix was incubated with the indicated antibodies for 1 h on ice before separating it by electrophoresis. Normal serum was used as a negative control.

2.17. Statistics

All experiments were repeated 3 times and data are presented as mean ± standard deviation (SD). The treatment effects were analyzed by One-way ANOVA and Bonferroni multiple comparison test and p values <0.05 were considered statistically significant. In the case of ChIP, EMSA, supershift EMSA, Western blots, immunofluorescence & fluorescence staining, one data set is presented.

3. Results

3.1. CREB Mediates VEGFC-Induced Sprouting and Tube Formation In vitro and Hypoxia-Induced Retinal Neovascularization In vivo

Current anti-angiogenic therapies are focused mostly on VEGFA neutralization or blockade of its signaling. However, a number of patients suffering from age-related macular degeneration or cancer do not respond to anti-VEGFA therapies (Jubb and Harris, 2010; Lux et al., 2007). Anti-VEGFA therapies have also been reported to cause tractional retinal detachments (Arevalo et al., 2008; Kuiper et al., 2008). Due to these reasons, we examined for VEGFA-related molecules that may influence angiogenesis and found that hypoxia induces the expression of VEGFC as robustly as VEGFA or VEGFB and VEGFD to a modest level in mouse retina (Fig. 1A). As we have previously reported a role for both VEGFA and VEGFB in retinal neovascularization (Singh et al., 2013) and hypoxia induces VEGFC as robustly as VEGFA, in the present study we have focused on the role of VEGFC in retinal neovascularization. VEGFC stimulated proliferation, migration and tube formation of HRMVECs (Fig. 1B-D). Since a role for CREB in tumor angiogenesis has been demonstrated (Abramovitch et al., 2004) and as nothing is known on its role in developmental or pathological retinal angiogenesis, we asked the question whether VEGFC activates this leucine-zipper transcriptional factor in mediating HRMVEC proliferation, migration and tube formation. VEGFC induced the phosphorylation of CREB in a time-dependent manner in HRMVECs (Fig. 1E). In addition, adenoviral-mediated expression of KCREB, the dominant negative mutant of CREB, attenuated VEGFC-induced proliferation, migration and tube formation of HRMVECs (Fig. 1F–I). Since sprouting is required for tubulogenesis, we also tested the effect of VEGFC on HRMVEC sprouting. VEGFC induced HRMVEC sprouting in a manner that is also sensitive to inhibition of CREB (Fig. 1J). Together, these data demonstrate that VEGFC induces HRMVEC proliferation, migration, sprouting and tubulogenesis and CREB mediates these effects. To validate these observations in vivo, we used oxygen-induced retinopathy (OIR) model. VEGFC down regulation using its siRNA inhibited hypoxia-induced retinal EC proliferation as observed by a decrease in the number of CD31 and Ki67-positive cells, the former being a marker for ECs and the latter being a marker for proliferating cells (Fig. 2A & B). In addition, blockade of VEGFC expression attenuated hypoxia-induced retinal EC filopodia formation suggesting its possible role in tip cell formation (Fig. 2C). Down regulation of VEGFC levels also attenuated hypoxia-induced expression of VEGFR3 (Fig. 2D), a marker for tip cells (Nicoli et al., 2012). Consistent with these observations, down regulation of VEGFC inhibited neovascularization with a reduction in tufts and anastomoses (Fig. 2E–G). Since phosphorylation at Ser133 is required for CREB activation (Arany et al., 1994; Chrivia et al., 1993), we next examined the effect of hypoxia on CREB phosphorylation. Hypoxia induced CREB phosphorylation in a time-dependent manner in mouse retina with maximum effect at 24 h and declining thereafter (Fig. 3A). Double

Fig. 3. CREB mediates hypoxia-induced retinal neovascularization. A. An equal amount of protein from normoxic and various time periods of hypoxic retinal extracts were analyzed by Western blotting for pCREB levels using its phospho-specific antibody and normalized to CREB. B. Following exposure to hyperoxia from P7 to P12, pups were returned to room air and at P15 the retinas were isolated, fixed, cross-sections were made and stained by immunofluorescence for CD31 and pCREB. C. All the conditions were the same as in panel B except that pups were administered intravitreally with 1 μg/0.5 μl/eye of control or VEGFC siRNA at P10 and P11 and at P13 the retinas were isolated and tissue extracts were prepared. An equal amount of protein from normoxic and hypoxic retinal extracts was analyzed by Western blotting for pCREB and CREB levels as described in panel A and the blot was reprobed for VEGFC or β-tubulin levels to show the effects of the siRNA on its target and off-target molecules, respectively. D. All the conditions were the same as in panel C except that pups were administered intravitreally with 1 μg/0.5 μl/eye of control or VEGFC siRNA at P12 and P13 and that at P15 the retinas were isolated and processed for CD31 and Ki67 immunofluorescence staining as described in Fig. 2, panel A. The right column shows the higher magnification (40×) of the areas selected by rectangular boxes in the images shown in the left column. E. Retinal EC proliferation was measured by counting CD31- and Ki67-positive cells that extended anterior to the inner limiting membrane per section (n = 6 eyes, 3 sections/eye). F. All the conditions were the same as in panel D except that control or CREB siRNAs were injected intravitreally at P12, P13, and P15 and at P17 the retinas were isolated, stained with isolectin B4, flat mounts were made and examined for EC filopodia formation at 40× magnification. G. All the conditions were the same as in panel D except that the sections were stained for CD31, VEGFR3 and DAPI. H. All the conditions were the same as in panel F except that retinal neovascularization was measured at 2.5× magnification. Retinal vascularization is shown in the first column. Neovascularization is highlighted in red in the second column. The third row shows the selected rectangular areas of the images shown in the first column under 10× magnification. I & J. Retinal neovascularization (I) and avascular areas (J) were determined as described in "Materials and Methods." The bar graphs represent quantitative analysis of three blots or 6 retinas. The values are presented as Mean ± SD. * $p < 0.01$ vs normoxia or normoxia + control siRNA; ** $p < 0.01$ vs hypoxia + control siRNA; § $p < 0.05$ vs hypoxia + control siRNA. Scale bar represents 50 μm and 20 μm in panels B & D, far left column and far right column, respectively, 20 μm in panels F & G, 300 μm and 50 μm in panel H, far left column and far right column, respectively.

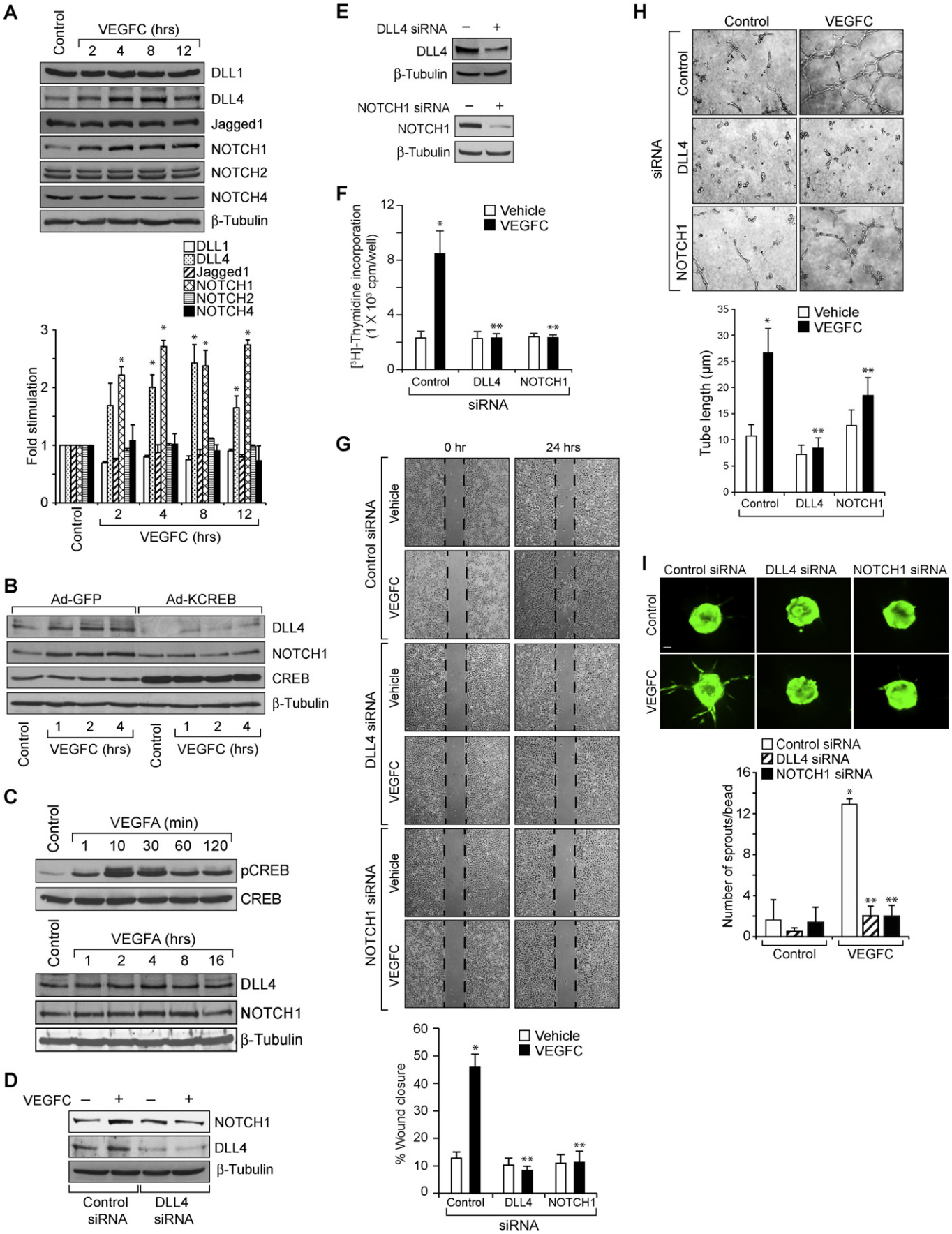
A
Control
VEGFC (hrs)
2 4 8 12
DLL1
DLL4
Jagged1
NOTCH1
NOTCH2
NOTCH4
β-Tubulin
DLL1
DLL4
Jagged1
NOTCH1
NOTCH2
NOTCH4
Fold stimulation
Control
VEGFC (hrs)
B
Ad-GFP
Ad-KCREB
DLL4
NOTCH1
CREB
β-Tubulin
Control
1 2 4
VEGFC (hrs)
C
Control
VEGFA (min)
1 10 30 60 120
pCREB
CREB
VEGFA (hrs)
1 2 4 8 16
DLL4
NOTCH1
β-Tubulin
D
VEGFC – + – +
NOTCH1
DLL4
β-Tubulin
Control siRNA
DLL4 siRNA
E
DLL4 siRNA – +
DLL4
β-Tubulin
NOTCH1 siRNA – +
NOTCH1
β-Tubulin
F
[3H]-Thymidine incorporation (1 X 10³ cpm/well)
Vehicle
VEGFC
Control
DLL4
NOTCH1
siRNA
G
0 hr
24 hrs
Control siRNA
DLL4 siRNA
NOTCH1 siRNA
Vehicle
VEGFC
% Wound closure
H
Control
VEGFC
siRNA
Control
DLL4
NOTCH1
Tube length (μm)
I
Control siRNA
DLL4 siRNA
NOTCH1 siRNA
Control
VEGFC
Number of sprouts/bead

immunofluorescence staining for CD31 and pCREB revealed that hypoxia induces CREB phosphorylation mostly in retinal ECs (Fig. 3B). In addition, down regulation of VEGFC substantially blocked hypoxia-induced CREB phosphorylation (Fig. 3C). Depletion of CREB levels using its siRNA also attenuated retinal EC proliferation, filopodia formation, VEGFR3 expression and neovascularization with more extensive vaso-obliteration (Fig. 3D–J).

3.2. CREB Modulates VEGFC-Induced Activation of DLL4-NOTCH1 Signaling

Previously, it has been reported that VEGFC activates VEGFR3 in tip cells to activate NOTCH signaling in the neighboring ECs leading to their phenotypic conversion to stalk cells (Tammela et al., 2008). Our data demonstrates that VEGFC mediates CREB activation both in vitro and in vivo. In addition, blockade of CREB activation led to a decrease in VEGFC-induced HRMVEC sprouting and tubulogenesis in vitro and retinal EC proliferation, filopodia formation, VEGFR3 expression and neovascularization in vivo. Based on these findings, we hypothesized that VEGFC might be activating NOTCH signaling requiring CREB. To test this, we have studied the time course effect of VEGFC on NOTCH signaling in HRMVECs. VEGFC while having no major effect on the steady state levels of DLL1, Jagged1, cleaved NOTCH2 and cleaved NOTCH4, increased the expression of DLL4 and augmented the production of cleaved NOTCH1 (cNOTCH1) levels in HRMVECs (Fig. 4A). In order to find the link between CREB and DLL4-NOTCH1 signaling, we tested the effect of KCREB on VEGFC-induced DLL4 expression and cleaved NOTCH1 levels. Adenoviral-mediated expression of KCREB blocked VEGFC-induced DLL4 expression and cleaved NOTCH1 production in HRMVECs (Fig. 4B). As VEGFA also activates CREB (Evans et al., 2010), we wanted to find whether VEGFA has any effect on DLL4 expression and cNOTCH1 levels in HRMVECs. VEGFA while stimulating CREB phosphorylation, had no apparent effect on DLL4 expression or cNOTCH1 levels (Fig. 4C). To find a link between DLL4 and cNOTCH1, we tested the effect of DLL4 siRNA on VEGFC-induced cNOTCH1 levels. Down regulation of DLL4 attenuated VEGFC-induced cNOTCH1 levels (Fig. 4D). Having found that CREB mediates VEGFC-induced DLL4-NOTCH1 signaling, we next investigated the effects of DLL4 and NOTCH1 on VEGFC-induced tube formation and sprouting. Knockdown of either DLL4 or NOTCH1 levels with their respective siRNA molecules reduced VEGFC-induced proliferation, migration, tube formation and sprouting (Fig. 4E–I). Together, these data provide compelling evidence that CREB mediates VEGFC-induced DLL4 expression and NOTCH1 activation leading to EC proliferation, migration, sprouting and tubulogenesis.

To understand the molecular mechanisms by which CREB regulates VEGFC-induced DLL4 expression, we cloned a ~ 2.21 kb human DLL4 promoter and identified two putative CREB binding sites, one at −193 nt and the other at −2026 nt by TRANSFAC analysis (Fig. 5A). The full-length 2.2 kb and a truncated region consisting of from −605 nt to +78 nt DLL4 promoter sequences were sub-cloned into pGL3 basic vector, transfected HRMVECs, treated with and without VEGFC for 4 h and the luciferase activity was measured. VEGFC induced a 6-fold increase in the luciferase activity with both full-length pGL3-hDLL4 (2.2 kb) and truncated pGL3-hDLL4 (0.68 kb) promoter constructs (Fig. 5B), suggesting that CREB element at −193 nt is sufficient for VEGFC-induced DLL4 promoter activity. To confirm these observations, we also studied a time course effect of VEGFC on CREB–DNA-binding activity by EMSA using CREB binding element at −193 nt as a biotin-labeled double-stranded oligonucleotide probe. VEGFC induced CREB–DNA-binding activity in a time-dependent manner with near maximum effect at 2 h (Fig. 5C). Furthermore, super-shift EMSA using anti-CREB antibodies confirmed the presence of CREB in DLL4 promoter DNA-protein complexes (Fig. 5C). In addition, ChIP analysis revealed a time-dependent binding of CREB to DLL4 promoter in response to VEGFC *in vivo* as well (Fig. 5D). Supporting these observations, site-directed mutagenesis of CREB element at −193 nt significantly reduced VEGFC-induced DLL4 promoter activity (Fig. 5E).

To test whether CREB modulates DLL4–NOTCH1 signaling in vivo, we studied the effect of hypoxia on DLL4 expression and cNOTCH1 generation. Hypoxia with little or no effect on DLL1 and Jagged1 levels induced DLL4 expression in the mouse retina (Fig. 6A). We also observed that hypoxia increases cNOTCH1 production with little or no effect on cNOTCH2 or cNOTCH4 levels (Fig. 6A). Furthermore, depletion of either VEGFC or CREB levels attenuated hypoxia-induced DLL4 expression and cNOTCH1 generation (Fig. 6B). Next, we studied the role of DLL4–NOTCH1 signaling in retinal neovascularization. Down regulation of either DLL4 or NOTCH1 levels resulted in decreased retinal EC proliferation, filopodia formation and VEGFR3 expression (Fig. 6C–F). Consistent with these observations, depletion of DLL4 or NOTCH1 levels also caused a marked decrease in vessel anastomoses and retinal neovascularization with more extensive vaso-obliteration as compared to controls (Fig. 6G–I). These results imply that blockade of DLL4–NOTCH1 signaling decreases tip cell formation and as a result of this affects stalk cell differentiation, thereby decreasing the vessel anastomoses.

3.3. Conditional Deletion of CREB Suppresses DLL4-NOTCH1 Activation and Retinal Neovascularization

To obtain additional support on the role of CREB in NOTCH1 activation and retinal neovascularization, we investigated the consequences of homozygous endothelial-specific loss of CREB during OIR. EC-specific deletion of CREB was achieved in $CREB^{flox/flox}$:Cdh5-CreERT2 mice by 2 consecutive intraperitoneal injections of tamoxifen on P10 and P11 (Fig. 7A). Cdh5-CreERT2 mice injected with two consecutive injections of tamoxifen were used as WT control. As shown in Fig. 7A, some residual CREB was detected in retinal extracts by Western blotting when Cre was induced in $CREB^{flox/flox}$:Cdh5-CreERT2 ($CREB^{i\Delta EC}$) mice, presumably due to other cell types such as retinal muller glial cell CREB. At P13, $CREB^{i\Delta EC}$ pups exhibited a significant decrease in hypoxia-induced DLL4 expression and cNOTCH1 production (Fig. 7B), indicating that CREB contributes to activation of NOTCH1 signaling in hypoxic retina. $CREB^{i\Delta EC}$ pups also showed a significant decrease in retinal EC proliferation, filopodia formation and neovascularization with extensive vaso-obliteration as compared to WT pups (Fig. 7C–H).

Fig. 4. DLL4 and NOTCH1 mediate VEGFC-induced angiogenic events. A. An equal amount of protein from control and various time periods of VEGFC (100 ng/ml)-treated HRMVECs were analyzed by Western blotting for DLL1, DLL4, Jagged1, NOTCH1, NOTCH2 and NOTCH4 levels using their specific antibodies. The DLL4 blot was normalized to β-tubulin. B. Cells were transduced with Ad-GFP or Ad-KCREB (40 moi), growth-arrested, treated with and without VEGFC (100 ng/ml) for the indicated time periods and cell extracts were prepared and analyzed for DLL4 and NOTCH1 levels using their specific antibodies and the blot was sequentially reprobed for CREB, and β-tubulin levels to show the overexpression of KCREB and normalization. C. An equal amount of protein from control and various time periods of VEGFA (40 ng/ml)-treated HRMVECs were analyzed by Western blotting for pCREB, CREB, DLL4 and cNOTCH1 levels using their specific antibodies and the DLL4 blot was normalized to β-tubulin. D. HRMVECs were transfected with control, or DLL4 siRNA, growth-arrested, treated with and without VEGFC (100 ng/ml) for 2 h, cell extracts were prepared and analyzed by Western blotting for NOTCH1 and DLL4 levels using their specific antibodies and normalized to β-tubulin. E. HRMVECs were transfected with control, DLL4 or NOTCH1 siRNA and 48 h later either cell extracts were prepared and analyzed by Western blotting for DLL4 and NOTCH1 levels using their specific antibodies and normalized to β-tubulin. F–H. All the conditions were the same as in panel E except that after transfection, cells were quiesced and subjected to VEGFC (100 ng/ml)-induced DNA synthesis (F), migration (G), or tube formation (H). I. All the conditions were the same as in panel E except that after transfection cells were subjected to sprouting assay as described in Fig. 1, panel J. The bar graphs represent quantitative analysis of 3 independent experiments. The values are presented as Mean ± SD. * $p < 0.01$ vs control; ** $p < 0.01$ vs control siRNA + VEGFC. Scale bar represents 50 μm in panel F.

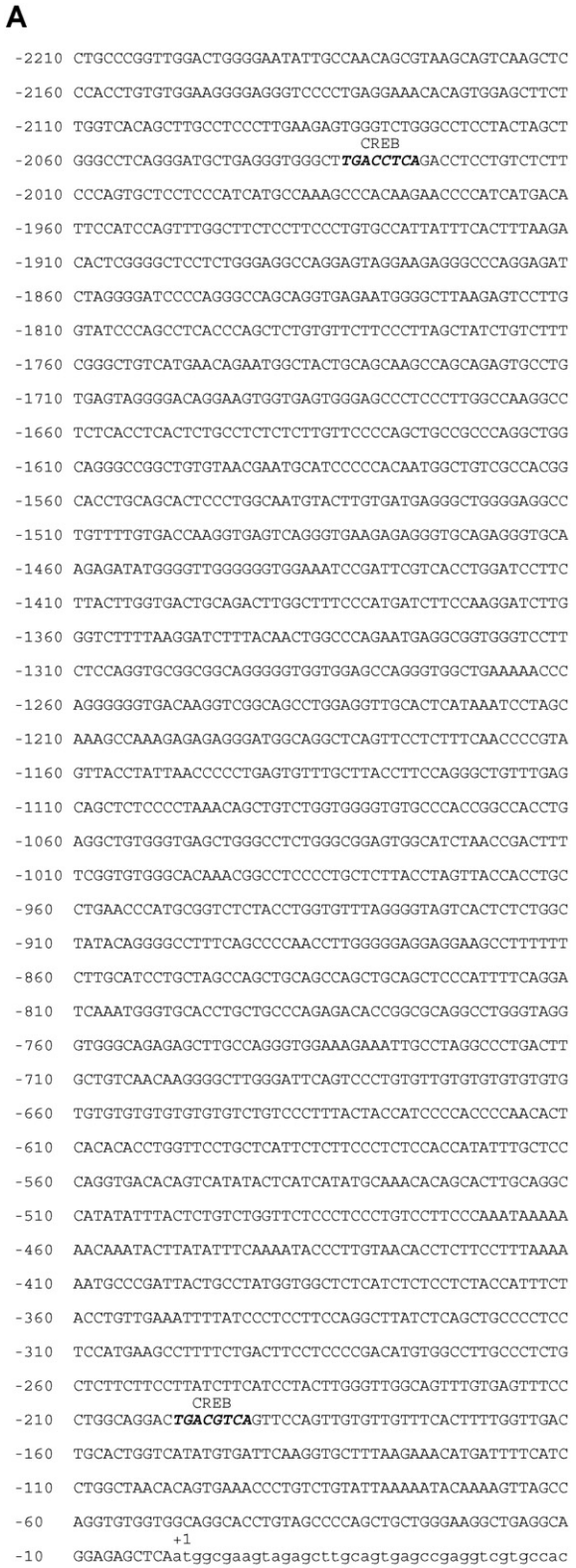
A
-2210 CTGCCCGGTTGGACTGGGGAATATTGCCAACAGCGTAAGCAGTCAAGCTC
-2160 CCACCTGTGTGGAAGGGGAGGGTCCCCTGAGGAAACACAGTGGAGCTTCT
-2110 TGGTCACAGCTTGCCTCCCTTGAAGAGTGGGTCTGGGCCTCCTACTAGCT
CREB
-2060 GGGCCTCAGGGATGCTGAGGGTGGGCTTGACCTCAGACCTCCTGTCTCTT
-2010 CCCAGTGCTCCTCCCATCATGCCAAAGCCCACAAGAACCCCATCATGACA
-1960 TTCCATCCAGTTTGGCTTCTCCTTCCCTGTGCCATTATTTCACTTTAAGA
-1910 CACTCGGGGCTCCTCTGGGAGGCCAGGAGTAGGAAGAGGGCCCAGGAGAT
-1860 CTAGGGGATCCCCAGGGCCAGCAGGTGAGAATGGGGCTTAAGAGTCCTTG
-1810 GTATCCCAGCCTCACCCAGCTCTGTGTTCTTCCCTTAGCTATCTGTCTTT
-1760 CGGGCTGTCATGAACAGAATGGCTACTGCAGCAAGCCAGCAGAGTGCCTG
-1710 TGAGTAGGGGACAGGAAGTGGTGAGTGGGAGCCCTCCCTTGGCCAAGGCC
-1660 TCTCACCTCACTCTGCCTCTCTCTTGTTCCCCAGCTGCCGCCCAGGCTGG
-1610 CAGGGCCGGCTGTGTAACGAATGCATCCCCCACAATGGCTGTCGCCACGG
-1560 CACCTGCAGCACTCCCTGGCAATGTACTTGTGATGAGGGCTGGGGAGGCC
-1510 TGTTTTGTGACCAAGGTGAGTCAGGGTGAAGAGAGGGTGCAGAGGGTGCA
-1460 AGAGATATGGGGTTGGGGGGTGGAAATCCGATTCGTCACCTGGATCCTTC
-1410 TTACTTGGTGACTGCAGACTTGGCTTTCCCATGATCTTCCAAGGATCTTG
-1360 GGTCTTTTAAGGATCTTTACAACTGGCCCAGAATGAGGCGGTGGGTCCTT
-1310 CTCCAGGTGCGGCGGCAGGGGGTGGTGGAGCCAGGGTGGCTGAAAAACCC
-1260 AGGGGGGTGACAAGGTCGGCAGCCTGGAGGTTGCACTCATAAATCCTAGC
-1210 AAAGCCAAAGAGAGAGGGATGGCAGGCTCAGTTCCTCTTTCAACCCCGTA
-1160 GTTACCTATTAACCCCCTGAGTGTTTGCTTACCTTCCAGGGCTGTTTGAG
-1110 CAGCTCTCCCCTAAACAGCTGTCTGGTGGGGTGTGCCCACCGGCCACCTG
-1060 AGGCTGTGGGTGAGCTGGGCCTCTGGGCGGAGTGGCATCTAACCGACTTT
-1010 TCGGTGTGGGCACAAACGGCCTCCCCTGCTCTTACCTAGTTACCACCTGC
-960 CTGAACCCATGCGGTCTCTACCTGGTGTTTAGGGGTAGTCACTCTCTGGC
-910 TATACAGGGGCCTTTCAGCCCCAACCTTGGGGGAGGAGGAAGCCTTTTTT
-860 CTTGCATCCTGCTAGCCAGCTGCAGCCAGCTGCAGCTCCCATTTTCAGGA
-810 TCAAATGGGTGCACCTGCTGCCCAGAGACACCGGCGCAGGCCTGGGTAGG
-760 GTGGGCAGAGAGCTTGCCAGGGTGGAAAGAAATTGCCTAGGCCCTGACTT
-710 GCTGTCAACAAGGGGCTTGGGATTCAGTCCCTGTGTTGTGTGTGTGTG
-660 TGTGTGTGTGTGTGTCTGTCCCTTTACTACCATCCCCACCCCAACACT
-610 CACACACCTGGTTCCTGCTCATTCTCTTCCCTCTCCACCATATTTGCTCC
-560 CAGGTGACACAGTCATATACTCATCATATGCAAACACAGCACTTGCAGGC
-510 CATATATTTACTCTGTCTGGTTCTCCCTCCCTGTCCTTCCCAAATAAAAA
-460 AACAAATACTTATATTTCAAAATACCCTTGTAACACCTCTTCCTTTAAAA
-410 AATGCCCGATTACTGCCTATGGTGGCTCTCATCTCTCCTCTACCATTTCT
-360 ACCTGTTGAAATTTTATCCCTCCTTCCAGGCTTATCTCAGCTGCCCCTCC
-310 TCCATGAAGCCTTTTCTGACTTCCTCCCCGACATGTGGCCTTGCCCTCTG
-260 CTCTTCTTCCTTATCTTCATCCTACTTGGGTTGGCAGTTTGTGAGTTTCC
CREB
-210 CTGGCAGGACTGACGTCAGTTCCAGTTGTGTTGTTTCACTTTTGGTTGAC
-160 TGCACTGGTCATATGTGATTCAAGGTGCTTTAAGAAACATGATTTTCATC
-110 CTGGCTAACACAGTGAAACCCTGTCTGTATTAAAAATACAAAAGTTAGCC
-60 AGGTGTGGTGGCAGGCACCTGTAGCCCCAGCTGCTGGGAAGGCTGAGGCA
+1
-10 GGAGAGCTCAatggcgaagtagagcttgcagtgagccgaggtcgtgccac
+38 tgcactccagcctgagtgacagagcaagactccgtctc
B
Control
VEGFC
RLU
200
150
100
50
0
*
*
pGL3
2.2 kb
0.68 kb
pGL3-hDLL4
C
Free probe
Control
VEGFC (min)
30
60
120
CREB-DNA complex
Free probe
IgG
CREB ab
VEGFC, 2 hrs
Supershift
D
Control
VEGFC (min)
30 60 120
220 bp
IgG + – + – + – + –
CREB ab – + – + – + – +
Input DNA
106 bp
Fold enrichment of CREB-bound DLL4 (106 bp) promter
25
20
15
10
5
0
E
Control
VEGFC
RLU
250
200
150
100
50
0
**
pGL3
2.2 kb
0.68 kb
pGL3-hDLL4

Collectively, these data indicate that CREB regulates DLL4–NOTCH1 signaling in modulating pathological retinal neovascularization.

3.4. p38MAPK Mediates VEGFC-Induced CREB-DLL4-NOTCH1 Activation in Retinal Neovascularization

Since CREB is activated by phosphorylation, we next examined for the upstream signaling events in VEGFC-induced CREB activation. VEGFC stimulated the phosphorylation of JNK1 and p38MAPK in a time-dependent manner in HRMVECs (Fig. 8A). While dominant negative mutant-mediated blockade of JNK1 activation had no effect, inhibition of p38MAPKβ by its dominant negative mutant suppressed VEGFC-induced CREB phosphorylation in HRMVECs (Fig. 8B). Because p38MAPKβ is involved in VEGFC-induced CREB activation, we further examined for its role in VEGFC-induced DLL4 expression and cNOTCH1 levels. Blockade of p38MAPKβ activation inhibited VEGFC-induced DLL4 expression and cNOTCH1 levels (Fig. 8C). Furthermore, inhibition of p38MAPKβ also attenuated VEGFC-induced proliferation, migration, tube formation and sprouting of HRMVECs (Fig. 8D–G). Having found that p38MAPKβ mediates VEGFC-induced CREB–DLL4–NOTCH1 signaling, we next studied its role in hypoxia-induced retinal neovascularization. Hypoxia induced p38MAPK activation as measured by its increased phosphorylation (Fig. 9A). In addition, siRNA-mediated down regulation of VEGFC levels attenuated hypoxia-induced p38MAPK phosphorylation suggesting that VEGFC mediates hypoxia-induced p38MAPK activation (Fig. 9B). Consistent with these observations, down regulation of p38MAPKβ levels inhibited hypoxia-induced CREB phosphorylation, DLL4 expression, cNOTCH1 levels, retinal EC proliferation, filopodia formation, VEGFR3 expression and neovascularization (Fig. 9C–I).

4. Discussion

Hypoxia and hypoxia-inducible factors are important cues in the modulation of retinal neovascularization (Arjamaa and Nikinmaa, 2006; Gariano and Gardner, 2005). It should be pointed out that hypoxia by itself provokes a constellation of signaling events that promote angiogenesis (Konisti et al., 2012; Semenza, 2003). Although a large body of evidence shows that VEGFA plays a major role in pathological retinal neovascularization (Carmeliet et al., 1996; Ferrara et al., 1996), the anti-VEGFA therapies have failed in the reduction of the overall severity of the disease and a number of patients suffering from age-related macular degeneration or cancer do not respond to these regimens (Jubb and Harris, 2010; Lux et al., 2007). In this regard, to understand the role of other molecules in the modulation of pathological retinal angiogenesis, we studied the capacity of VEGFA-related molecules. We found that hypoxia induces the expression of VEGFC as potently as VEGFA in the retina. Interestingly, VEGFC expression was also found in angiogenic ECs during retinal development (Tammela et al., 2008). VEGFC induces the proliferation, migration, sprouting and tube formation of HRMVECs, the findings suggesting its role in retinal angiogenesis. As CREB mediates hypoxia-induced expression of a number of growth factors (Kang et al., 2014; Leonard et al., 2008; Morishita et al., 1995; Wu et al., 2007) and its activity potentiates tumor angiogenesis (Abramovitch et al., 2004), we explored its role in VEGFC-induced HRMVEC proliferation, migration, sprouting and tube formation. Our results indicate that VEGFC stimulates CREB activation in HRMVECs. In addition, blockade of CREB activation by its dominant negative mutant blunted VEGFC-induced HRMVEC proliferation, migration, sprouting and tube formation. These findings infer that CREB mediates VEGFC-induced angiogenic events in HRMVECs. Although the involvement of CREB in tumor angiogenesis has been demonstrated (Abramovitch et al., 2004; Chen et al., 2005), its role in hypoxia-induced retinal neovascularization is not known. Therefore, as CREB mediates VEGFC-induced HRMVEC sprouting and tube formation, we next investigated the functional significance of VEGFC–CREB axis in retinal neovascularization. The observations that suppression of VEGFC levels attenuates hypoxia-induced retinal EC proliferation, tip cell formation and neovascularization suggest a role for VEGFC in pathological retinal neovascularizaion. VEGFC has also been reported to play a role in developmental and tumor angiogenesis (De Palma et al., 2003; Ober et al., 2004). Second, our findings show that hypoxia induces CREB activation in retina in VEGFC-dependent manner and suppression of its levels inhibits hypoxia-induced EC proliferation, tip cell formation and neovascularization.

To elucidate the mechanisms by which VEGFC–CREB axis plays a role in vessel formation, we investigated the effect of VEGFC and hypoxia on NOTCH signaling. Our in vitro and in vivo findings indicate that both VEGFC and hypoxia stimulate DLL4–NOTCH1 signaling and these events require the activation of CREB. In addition, hypoxia-induced DLL4–NOTCH1 activation depends on VEGFC production. Furthermore, the role of CREB in DLL4–NOTCH1 activation can be corroborated by the observations that CREB is essential for VEGFC-induced DLL4 promoter activity. It was noted that although VEGFA activated CREB in HRMVECs it failed to enhance DLL4 expression and cNOTCH1 production. Based on these findings, it may be suggested that activation of CREB alone is not sufficient for DLL4 expression and that VEGFC besides CREB also triggers the activation of additional signaling events, which in combination with CREB are required for DLL4 expression and cNOTCH1 production. The role of DLL4–NOTCH1 signaling in retinal neovascularization can be supported by the findings that depletion of DLL4 or NOTCH1 led to a decrease in VEGFC-induced proliferation, migration, tube formation and sprouting in vitro and EC proliferation, tip cell formation and neovacularization in vivo. The increase in avascular area in DLL4 and NOTCH1-depleted retina adds additional line of evidence for the role of NOTCH signaling in the regulation of tip cell formation. Indeed, other studies have also reported that NOTCH signaling plays a role in tip cell formation during angiogenesis (Hellstrom et al., 2007; Tammela et al., 2011). In addition, a reduction in EC proliferation, tip cells, tufts, and anastomoses in DLL4 or NOTCH1-depleted hypoxic retina support the observations of (Lobov et al. (2007, 2011) that genetic deletion of DLL4 or administration of DLL4-Fc suppresses pathological retinal neovascularization in OIR model. However, these authors reported that inhibition of DLL4–NOTCH signaling results in enhanced sprouting, which is contrary to our findings, as we did not observe any increase in tip cell formation in DLL4 or NOTCH1-depleted retinas. It should also be pointed out that many studies have demonstrated

Fig. 5. CREB is required for VEGFC-induced DLL4 promoter activity. A. DLL4 promoter encompassing −2210 nt to +78 nt was cloned and the nucleotide sequence with CREB binding sites highlighted in bold italic letters is shown. B. The full-length (from −2210 nt to +78 nt) and a truncated DLL4 promoter encompassing from −605 nt to +78 nt were sub-cloned into pGL3 vector yielding pGL3-hDLL4 (2.28 kb) and pGL3-hDLL4 (0.68 kb) plasmids. HRMVECs were transfected with empty vector or pGL3-hDLL4 (2.28 kb) or pGL3-hDLL4 (0.68 kb) promoter plasmid DNAs, growth-arrested, treated with vehicle or VEGFC for 4 h and the luciferase activity was measured. C. Left panel: Nuclear extracts of control and various time periods of VEGFC (100 ng/ml)-treated cells were analyzed by EMSA for CREB binding using CREB-binding site at −193 nt as a Biotin-labeled probe. Right panel: Nuclear extracts of control and 2 h of VEGFC (100 ng/ml)-treated cells were analyzed by supershift EMSA using normal IgG or anti-CREB antibodies. D. Control and various time periods of VEGFC (100 ng/ml)-treated cells were analyzed for CREB binding to DLL4 promoter by ChIP assay using two sets of primers that amplify a 220 bp and a 106 bp DNA fragments surrounding the CREB-binding site at −193 nt. The data in the bar graph in panel D represents the qPCR of 106 bp region of CREB-bound DLL4 promoter. E. HRMVECs were transfected with empty vector or pGL3-hDLL4 (0.68 kb) promoter plasmid DNA with and without the CREB-binding site mutated (TGA was mutated to CTC), growth-arrested, treated with and without VEGFC (100 ng/ml) for 4 h and the luciferase activity was measured. The bar graphs represent quantitative analysis of three independent experiments. The values represent Mean ± SD. * $p < 0.01$ vs control; ** $p < 0.01$ vs pGL3-hDLL4 (0.68 kb) + VEGFC.

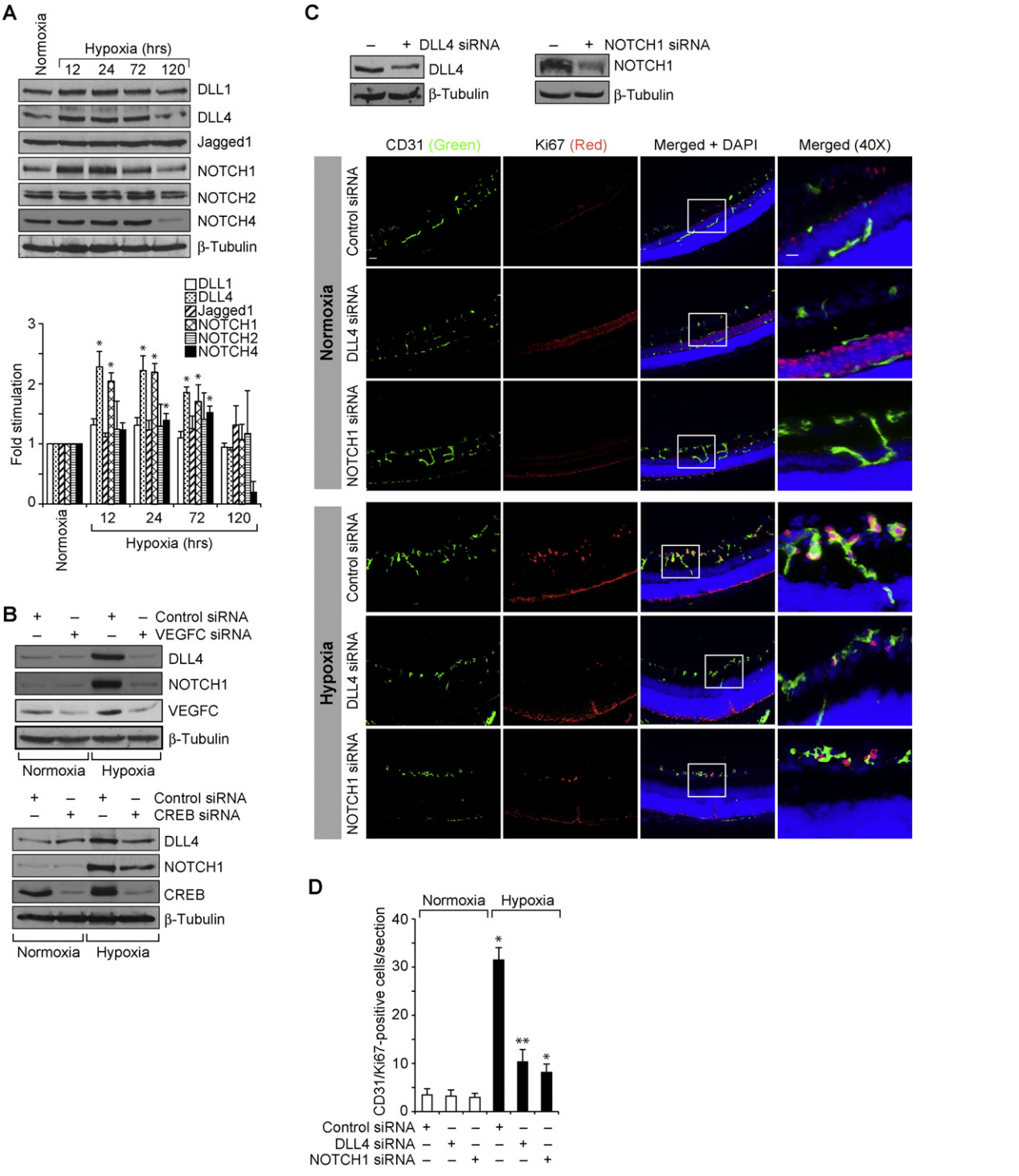

Fig. 6. CREB-mediated DLL4-NOTCH1 signaling is required for hypoxia-induced neovascularization. A. An equal amount of protein from normoxic and various time periods of hypoxic retinal extracts were analyzed by Western blotting for the indicated proteins using their specific antibodies and normalized to β-tubulin. B. All the conditions were the same as in panel A except that pups were administered intravitreally with 1 μg/0.5 μl/eye of scrambled, VEGFC or CREB siRNA at P10 and P11 and at P13 the retinas were isolated and tissue extracts were prepared. An equal amount of protein from normoxic and hypoxic retinal extracts were analyzed by Western blotting for the indicated proteins using their specific antibodies and normalized to β-tubulin. C. All the conditions were the same as in panel B except that pups were administered intravitreally with 1 μg/0.5 μl/eye of scrambled, DLL4 or NOTCH1 siRNA at P12 and P13 and at P15 retinas were isolated and either tissue extracts were prepared and analyzed by Western blotting for DLL4 and NOTCH1 levels and normalized to β-tubulin or cross-sections were made, fixed and stained by immunofluorescence for CD31 and Ki67. D. Retinal EC proliferation was measured by counting CD31- and Ki67-positive cells that extended anterior to the inner limiting membrane per section (n = 6 eyes, 3 sections/eye). E. All the conditions were the same as in panel D except that at P17 retinas were isolated, stained with isolectin B4 and flat mounts were made and examined for EC filopodia formation. F. All the conditions were the same as in panel C except that the sections were stained for CD31, VEGFR3 and DAPI. G. All the conditions were the same as in panel C except that pups were administered intravitreally with 1 μg/0.5 μl/eye of scrambled, DLL4 or NOTCH1 siRNA at P12, P13 and P15 and at P17 retinas were isolated, stained with isolectin B4, flat mounts were made and examined for neovascularization. Retinal vascularization is shown in the first row. Neovascularization is highlighted in red in the second row. The third row shows the selected rectangular areas of the images shown in the first row under 10X magnification. H & I. Retinal neovascularization (H) and avascular areas (I) were determined as described in "Materials and Methods." The bar graphs represent quantitative analysis of 6 retinas. The values are presented as Mean ± SD. * $p < 0.01$ vs normoxia, normoxia + control siRNA; ** $p < 0.01$ vs hypoxia + control siRNA. Scale bar represents 50 μm and 20 μm in panel C, far left column and far right column, respectively, 20 μm in panels E & F and 300 μm and 50 μm in panel G, upper row and bottom row, respectively.

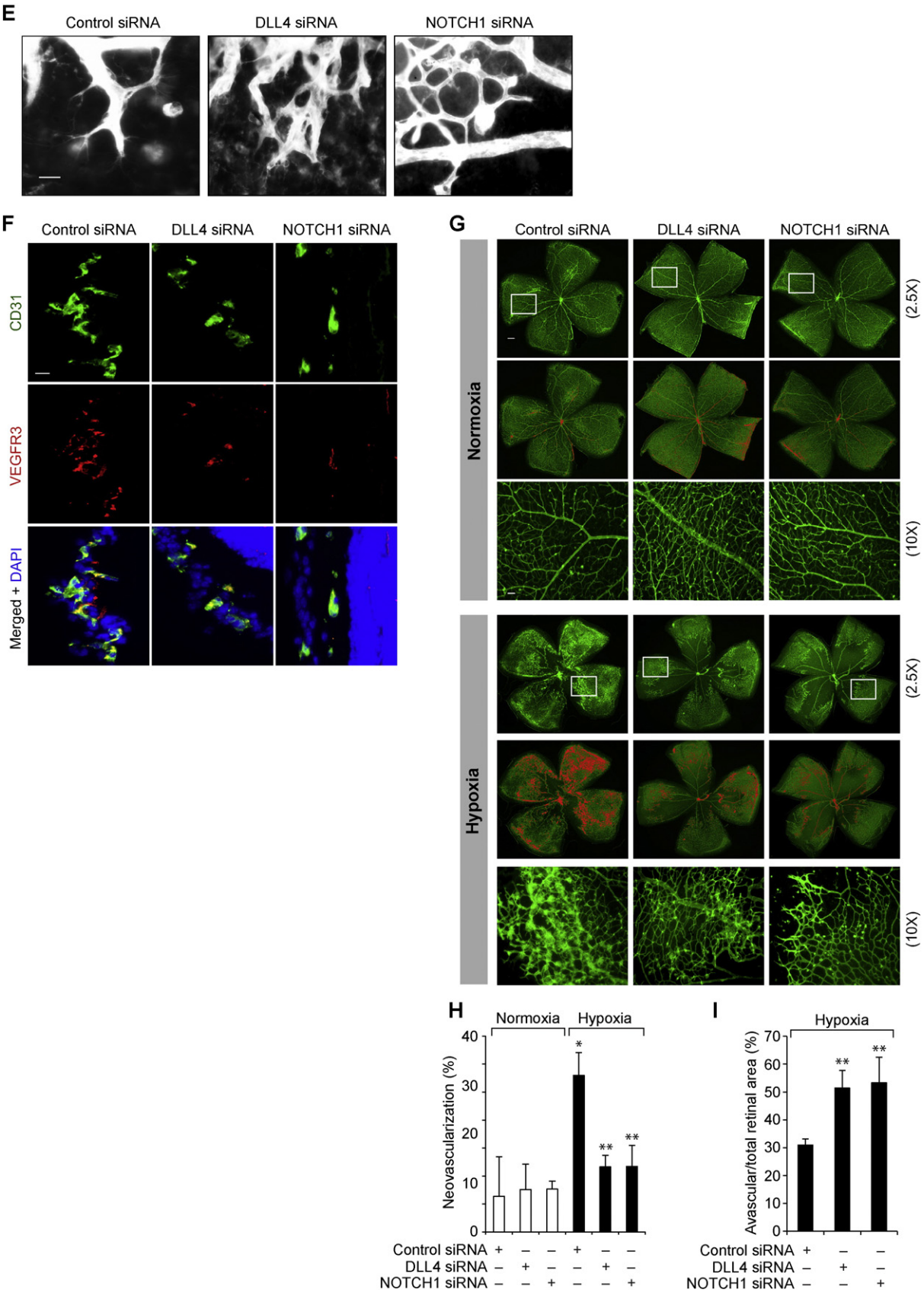

Fig. 6 (*continued*).

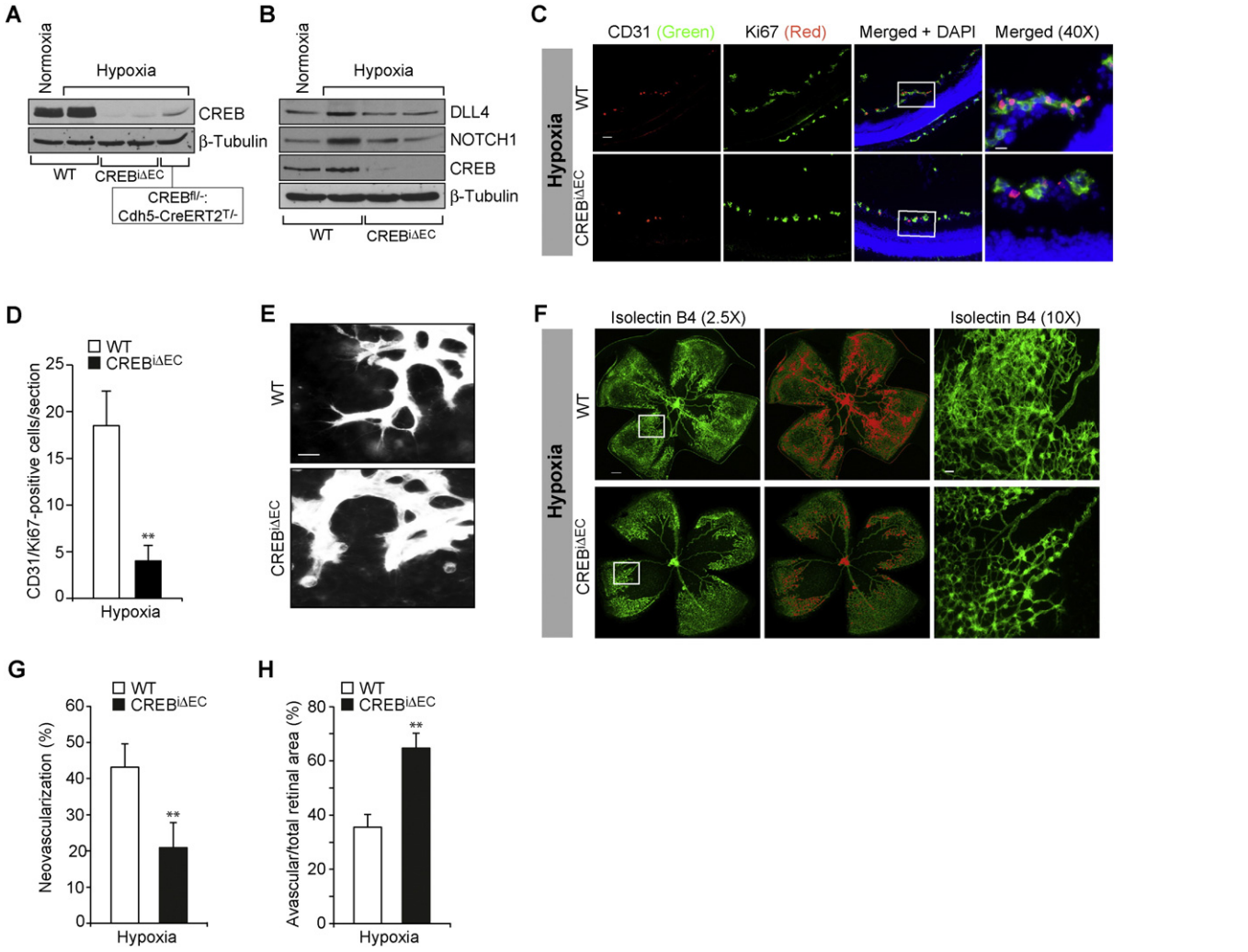

Fig. 7. Conditional knockout of CREB in EC attenuates DLL4–NOTCH1 signaling and retinal neovascularization. A. Tamoxifen was given intraperitoneally to CREB$^{fl/fl}$:Cdh5-CreERT2, and CREB$^{fl/-}$:Cdh5-CreERT2 pups on P10 and P11, when the pups were under hyperoxia and at P13 the retinas were isolated from WT (both from normoxia and hypoxia), CREB$^{i\Delta EC}$, and CREB$^{fl/-}$:Cdh5-CreERT2$^{T/-}$ pups, and extracts were prepared and an equal amount of protein from each group was analyzed by Western blotting for CREB using its specific antibody and normalized to β-tubulin. B. All the conditions were the same as in panel A except that the retinal extracts from WT, CREB$^{i\Delta EC}$ pups were analyzed by Western blotting for DLL4, NOTCH1 and CREB levels using their specific antibodies and normalized to β-tubulin. C & D. WT and CREB$^{i\Delta EC}$ mice pups after exposure to 75% oxygen from P7 to P12 were returned to normoxia to develop the relative hypoxia. At P15, the retinas were isolated, cross-sections were made and stained by immunofluorescence for CD31 and Ki67 (C) and cells positive for both CD31 and Ki67 were counted (D). E & F. All the conditions were the same as in panel C except that at P17 the retinas were isolated, stained with isolectin B4 and flat mounts were made and examined either for EC filopodia formation or neovascularization. In panel F, retinal vascularization is shown in the first column. Neovascularization is highlighted in red in the second column. The third column shows the selected rectangular areas of the images shown in the first column under 10X magnification. G & H. Retinal neovascularization (G) and avascular areas (H) were determined as described in "Materials and Methods." The bar graphs represent quantitative analysis of 6 retinas. The values are presented as Mean ± SD. * $p < 0.01$ vs WT. Scale bar represents 50 μm and 20 μm in panel C, far left column and far right column, respectively, 20 μm in panel E and 300 μm and 50 μm in panel F, far left column and far right column, respectively.

that inhibition of DLL4 or NOTCH1 levels results in excessive sprouting (Phng and Gerhardt, 2009) but reduces tumor growth (Noguera-Troise et al., 2006; Ridgway et al., 2006). It should also be pointed out that many reports show that the DLL4–NOTCH1 signaling negatively regulates EC proliferation, migration and tip cell formation while enhancing stalk cells (Hellstrom et al., 2007; Williams et al., 2006). On the other hand, our results show that the DLL4–NOTCH1 signaling enhances EC proliferation, migration and tip cell formation both in vitro in cell culture system and in vivo in hypoxic retina. A recent study also reported that the DLL4–NOTCH1 signaling via modulating TGFβ expression enhances tumor cell growth (Ohnuki et al., 2014), which is in line with our findings on the role of DLL4–NOTCH1 signaling in cell proliferation.

In order to validate the link between CREB and NOTCH in the regulation of pathological retinal angiogenesis, we employed inducible endothelial-specific CREB (CREB$^{i\Delta EC}$) knockout mice. First, EC-specific

Fig. 8. p38MAPKβ mediates VEGFC-induced angiogenic events. A. An equal amount of protein from control and various time periods of VEGFC (100 ng/ml)-treated HRMVECs were analyzed by Western blotting for pJNK1 and pp38MAPK levels using their phospho-specific antibodies and normalized to their total levels. B. Cells were transduced with Ad-GFP, Ad-JNK1 or Ad-dnp38MAPKβ (p38β) (40 moi), growth-arrested, treated with and without VEGFC (100 ng/ml) for 10 min and cell extracts were prepared and analyzed for pCREB levels using its phospho-specific antibodies and the blot was sequentially reprobed for CREB, JNK1, p38MAPK and β-tubulin levels to show the over expression of dnJNK1, dnp38β or normalization. C. Cells were transduced with Ad-GFP or Ad-dnp38β (40 moi), growth-arrested, treated with and without VEGFC (100 ng/ml) for 2 h and cell extracts were prepared and analyzed for DLL4 or cNOTCH1 levels using their specific antibodies and the blot was sequentially reprobed for p38β and β-tubulin to show the over expression of dnp38β or normalization. D–G. Cells were transduced with Ad-GFP or Ad-dnp38β (40 moi), growth-arrested and subjected to DNA synthesis (D), migration (E), tube formation (F) or sprouting assay (G). The bar graphs represent quantitative analysis of 3 independent experiments. The values are presented as Mean ± SD. * $p < 0.01$ vs control; ** $p < 0.01$ vs control siRNA + VEGFC. Scale bar represents 50 μm in panel E.

deletion of CREB in CREB$^{i\Delta EC}$ mice pups by tamoxifen led to decreased DLL4 expression and cNOTCH1 production in the hypoxic retina as compared to WT mice pups, a finding that shows the requirement of CREB in the regulation of DLL4–NOTCH1 signaling. Second, EC-specific deletion of CREB in CREB$^{i\Delta EC}$ mice pups also caused a decrease in ectopic growth of neovascular tufts and anastomoses with an increase in avascular area

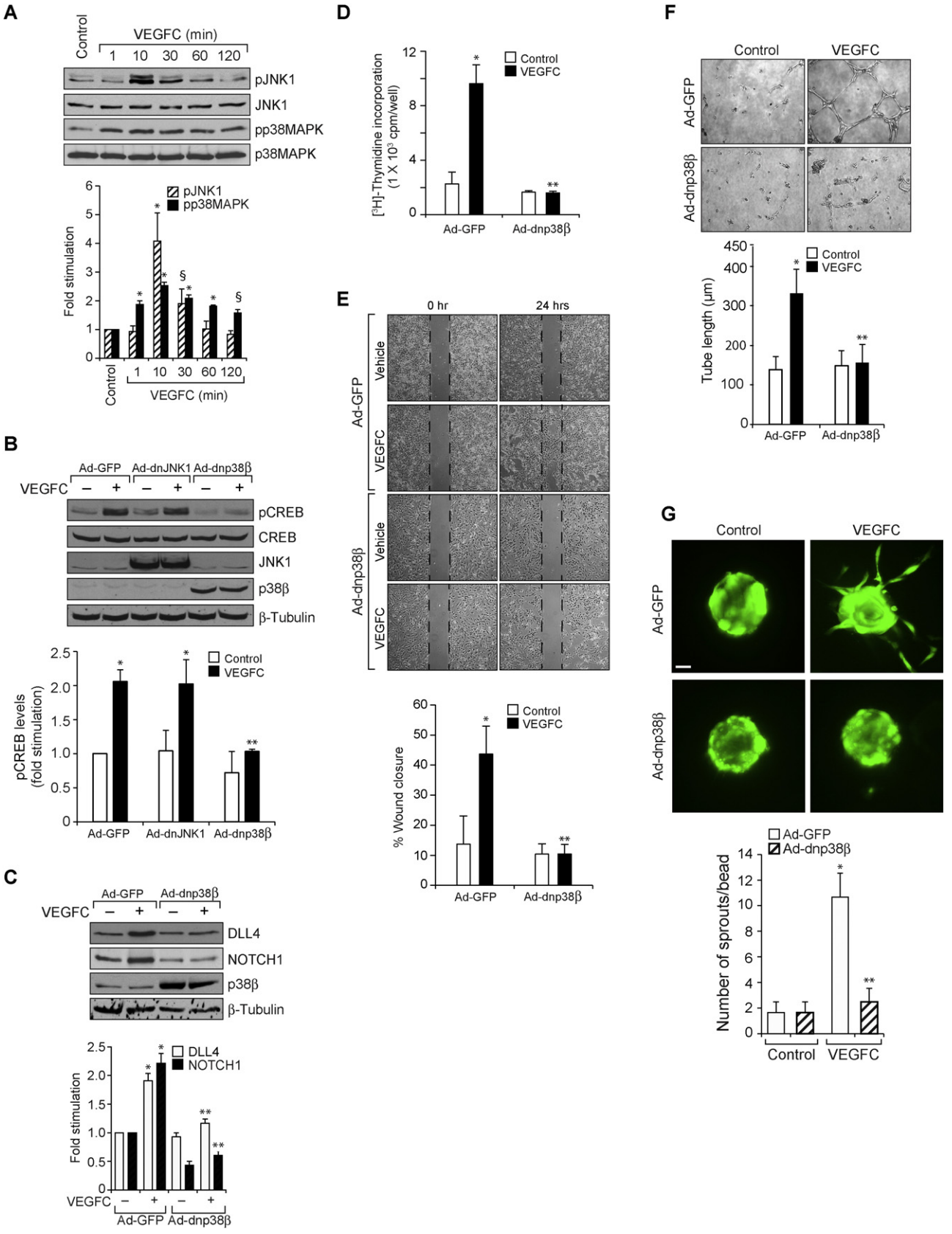

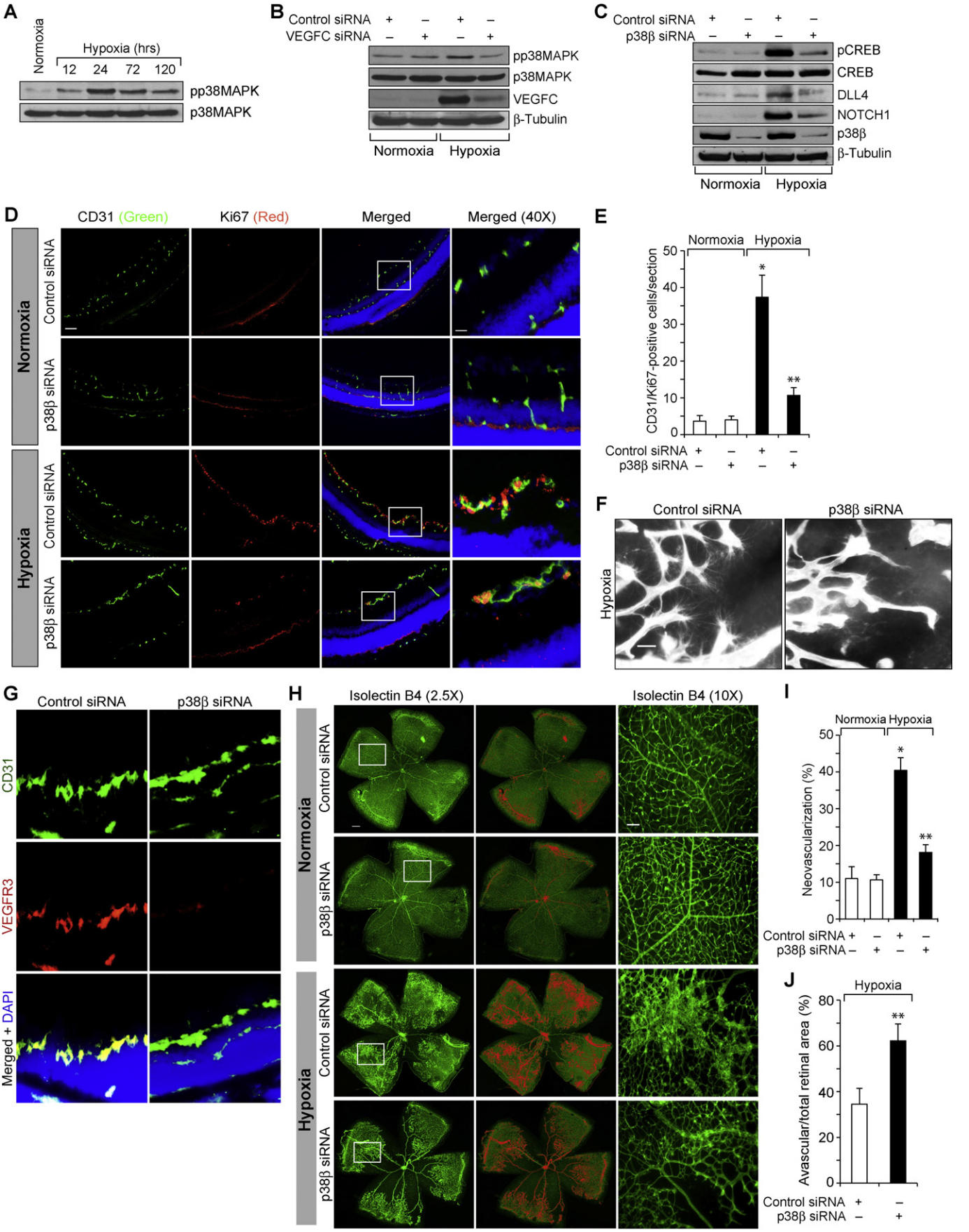
A
Normoxia
Hypoxia (hrs)
12 24 72 120
pp38MAPK
p38MAPK
B
Control siRNA + – + –
VEGFC siRNA – + – +
pp38MAPK
p38MAPK
VEGFC
β-Tubulin
Normoxia Hypoxia
C
Control siRNA + – + –
p38β siRNA – + – +
pCREB
CREB
DLL4
NOTCH1
p38β
β-Tubulin
Normoxia Hypoxia
D
CD31 (Green)
Ki67 (Red)
Merged
Merged (40X)
Normoxia
Hypoxia
Control siRNA
p38β siRNA
E
Normoxia Hypoxia
CD31/Ki67-positive cells/section
Control siRNA + – + –
p38β siRNA – + – +
F
Control siRNA
p38β siRNA
Hypoxia
G
Control siRNA
p38β siRNA
CD31
VEGFR3
Merged + DAPI
H
Isolectin B4 (2.5X)
Isolectin B4 (10X)
Normoxia
Hypoxia
Control siRNA
p38β siRNA
I
Normoxia Hypoxia
Neovascularization (%)
Control siRNA + – + –
p38β siRNA – + – +
J
Hypoxia
Avascular/total retinal area (%)
Control siRNA + –
p38β siRNA – +

in the hypoxic retina as compared to WT mice pups, and these observations attest that CREB–DLL4–NOTCH1 signaling plays a major role in pathological retinal neovascularization. Many reports have shown that MAPKs play a role in the activation of CREB in response to a variety of cues (Deak et al., 1998; Xing et al., 1998). In this context, our results reveal that p38MAPKβ mediates CREB phosphorylation in response to VEGFC in HRMVECs and hypoxia in the retina. In addition, activation of p38MAPKβ is required for VEGFC-induced DLL4 expression and cNOTCH1 production in HRMVECs facilitating their proliferation, migration, sprouting and tubulogenesis. Similarly, hypoxia induced p38MAPK activation in a manner that is dependent on VEGFC production and down regulation of p38MAPKβ levels attenuated hypoxia-induced CREB phosphorylation, DLL4 expression and cNOTCH1 production and, thereby, reducing retinal EC proliferation, tip cell formation, and neovascularization. Based on these findings, it may be suggested that p38MAPKβ via activation of CREB triggers DLL4–NOTCH1 signaling in enhancing EC proliferation, tip cell formation and retinal neovascularization. Retinal neovascularization is a leading cause of blindness in conditions such as diabetic retinopathy and retinopathy of pre-maturity. Presently, although anti-VEGFA therapy appears to be the major treatment for these ocular pathologies, such treatments have met with limitations (Arevalo et al., 2008; Kuiper et al., 2008). In this aspect, the present findings identify p38MAPKβ and CREB as potential targets in the development of therapeutic compounds in the amelioration of pathological retinal neovascularization. Based on the present and previous observations, therapies that target both VEGFA and VEGFC might also prove to be more efficacious in treating retinopathies.

Funding

This work was supported by a grant EY014856 to GNR from National Eye Institute of the National Institutes of Health.

Authors' Contributions

NKS, performed cell migration, DNA synthesis, flat mounts, immunohistochemistry, immunofluorescence staining, retinal angiogenesis, sprouting, tube formation, Western blot analysis, and wrote the draft manuscript; SK, performed cloning, EMSA, supershift EMSA, mutagenesis and promoter-reporter gene assays; RK, peformed tube formation and Western blotting analysis; GNR, conceived the overall scope of the project, interpreted the data and wrote the manuscript.

Conflict of Interest

None.

References

Abramovitch, R., Tavor, E., Jacob-Hirsch, J., Zeira, E., Amariglio, N., Pappo, O., Rechavi, G., Galun, E., Honigman, A., 2004. A pivotal role of cyclic amp-responsive element binding protein in tumor progression. Cancer Res. 64, 1338–1346.

Achen, M.G., Jeltsch, M., Kukk, E., Makinen, T., Vitali, A., Wilks, A.F., Alitalo, K., Stacker, S.A., 1998. Vascular Endothelial Growth Factor D (VEGF-D) is a ligand for the tyrosine kinases VEGF receptor 2 (Flk1) and VEGF receptor 3 (Flt4). Proc. Natl. Acad. Sci. U. S. A. 95, 548–553.

Aiello, L.P., Avery, R.L., Arrigg, P.G., Keyt, B.A., Jampel, H.D., Shah, S.T., Pasquale, L.R., Thieme, H., Iwamoto, M.A., Park, J.E., Nguyen, H.V., Aiello, L.M., Ferrara, N., King, G.L., 1994. Vascular endothelial growth factor in ocular fluid of patients with diabetic retinopathy and other retinal disorders. N. Engl. J. Med. 331, 1480–1487.

Alon, T., Hemo, I., Itin, A., Pe'er, J., Stone, J., Keshet, E., 1995. Vascular endothelial growth factor acts as a survival factor for newly formed retinal vessels and has implications for retinopathy of prematurity. Nat. Med. 1, 1024–1028.

Andreoli, C.M., Miller, J.W., 2007. Anti-vascular endothelial growth factor therapy for ocular neovascular disease. Curr. Opin. Ophthalmol. 18, 502–508.

Arany, Z., Sellers, W.R., Livingston, D.M., Eckner, R., 1994. E1A-associated p300 and CREB-associated CBP belong to a conserved family of coactivators. Cell 77, 799–800.

Arevalo, J.F., Maia, M., Flynn Jr., H.W., Saravia, M., Avery, R.L., Wu, L., Eid Farah, M., Pieramici, D.J., Berrocal, M.H., Sanchez, J.G., 2008. Tractional retinal detachment following intravitreal bevacizumab (Avastin) in patients with severe proliferative diabetic retinopathy. Br. J. Ophthalmol. 92, 213–216.

Arjamaa, O., Nikinmaa, M., 2006. Oxygen-dependent diseases in the retina: role of hypoxia-inducible factors. Exp. Eye Res. 83, 473–483.

Cao, Y., Linden, P., Farnebo, J., Cao, R., Eriksson, A., Kumar, V., Qi, J.H., Claesson-Welsh, L., Alitalo, K., 1998. Vascular endothelial growth factor C induces angiogenesis in vivo. Proc. Natl. Acad. Sci. U. S. A. 95, 14389–14394.

Carmeliet, P., Ferreira, V., Breier, G., Pollefeyt, S., Kieckens, L., Gertsenstein, M., Fahrig, M., Vandenhoeck, A., Harpal, K., Eberhardt, C., Declercq, C., Pawling, J., Moons, L., Collen, D., Risau, W., Nagy, A., 1996. Abnormal blood vessel development and lethality in embryos lacking a single VEGF allele. Nature 380, 435–439.

Chen, J., Smith, L.E., 2007. Retinopathy of prematurity. Angiogenesis 10, 133–140.

Chen, A.E., Ginty, D.D., Fan, C.M., 2005. Protein kinase A signalling via CREB controls myogenesis induced by Wnt proteins. Nature 433, 317–322.

Chrivia, J.C., Kwok, R.P., Lamb, N., Hagiwara, M., Montminy, M.R., Goodman, R.H., 1993. Phosphorylated CREB binds specifically to the nuclear protein CBP. Nature 365, 855–859.

Connor, K.M., Krah, N.M., Dennison, R.J., Aderman, C.M., Chen, J., Guerin, K.I., Sapieha, P., Stahl, A., Willett, K.L., Smith, L.E., 2009. Quantification of oxygen-induced retinopathy in the mouse: a model of vessel loss, vessel regrowth and pathological angiogenesis. Nat. Protoc. 4, 1565–1573.

De Palma, M., Venneri, M.A., Roca, C., Naldini, L., 2003. Targeting exogenous genes to tumor angiogenesis by transplantation of genetically modified hematopoietic stem cells. Nat. Med. 9, 789–795.

Deak, M., Clifton, A.D., Lucocq, L.M., Alessi, D.R., 1998. Mitogen- and stress-activated protein kinase-1 (MSK1) is directly activated by MAPK and SAPK2/p38, and may mediate activation of CREB. EMBO J. 17, 4426–4441.

Evans, I.M., Bagherzadeh, A., Charles, M., Raynham, T., Ireson, C., Boakes, A., Kelland, L., Zachary, I.C., 2010. Characterization of the biological effects of a novel protein kinase D inhibitor in endothelial Cells. Biochem. J. 429, 565–572.

Ferrara, N., Kerbel, R.S., 2005. Angiogenesis as a therapeutic target. Nature 438, 967–974.

Ferrara, N., Carver-Moore, K., Chen, H., Dowd, M., Lu, L., O'Shea, K.S., Powell-Braxton, L., Hillan, K.J., Moore, M.W., 1996. Heterozygous embryonic lethality induced by targeted inactivation of the VEGF gene. Nature 380, 439–442.

Gariano, R.F., Gardner, T.W., 2005. Retinal angiogenesis in development and disease. Nature 438, 960–966.

Hellstrom, M., Phng, L.K., Hofmann, J.J., Wallgard, E., Coultas, L., Lindblom, P., Alva, J., Nilsson, A.K., Karlsson, L., Gaiano, N., Yoon, K., Rossant, J., Iruela-Arispe, M.L., Kalen, M., Gerhardt, H., Betsholtz, C., 2007. Dll4 signalling through Notch1 regulates formation of tip cells during angiogenesis. Nature 445, 776–780.

Hoot, K.E., Oka, M., Han, G., Bottinger, E., Zhang, Q., Wang, X.J., 2010. HGF upregulation contributes to angiogenesis in mice with keratinocyte-specific Smad2 deletion. J. Clin. Invest. 120, 3606–3616.

Jeltsch, M., Kaipainen, A., Joukov, V., Meng, X., Lakso, M., Rauvala, H., Swartz, M., Fukumura, D., Jain, R.K., Alitalo, K., 1997. Hyperplasia of lymphatic vessels in VEGF-C transgenic mice. Science 276, 1423–1425.

Jubb, A.M., Harris, A.L., 2010. Biomarkers to predict the clinical efficacy of bevacizumab in cancer. Lancet Oncol. 11, 1172–1183.

Kaipainen, A., Korhonen, J., Mustonen, T., van Hinsbergh, V.W., Fang, G.H., Dumont, D., Breitman, M., Alitalo, K., 1995. Expression of the fms-Like tyrosine kinase 4 gene becomes restricted to lymphatic endothelium during development. Proc. Natl. Acad. Sci. U. S. A. 92, 3566–3570.

Kang, Z., Zhu, H., Luan, H., Han, F., Jiang, W., 2014. Curculigoside A induces angiogenesis through VCAM-1/Egr-3/CREB/VEGF signaling pathway. Neuroscience 267, 232–240.

Fig. 9. p38MAPKβ mediates hypoxia-induced CREB–DLL4–NOTCH1 activation and neovascularization. A. An equal amount of protein from normoxic and various time periods of hypoxic retinal extracts were analyzed by Western blotting for pp38MAPK levels using its phospho-specific antibodies and normalized to its total level. B & C. All the conditions were the same as in panel A except that pups were administered intravitreally with 1 μg/0.5 μl/eye of scrambled, VEGFC, or p38β siRNA at P10 and P11 and at P13 the retinas were isolated and tissue extracts were prepared. An equal amount of protein from normoxic and hypoxic retinal extracts were analyzed by Western blotting for the indicated proteins using their specific antibodies and normalized to β-tubulin. D. All the conditions were the same as in panel C except that pups were administered intravitreally with 1 μg/0.5 μl/eye of scrambled, or p38β siRNA at P12 and P13 and at P15 retinas were isolated, cross-sections were made and stained by immunofluorescence for CD31 and Ki67. E. Retinal EC proliferation was measured by counting CD31- and Ki67-positive cells that extended anterior to the inner limiting membrane per section ($n = 6$ eyes, 3 sections/eye). F. All the conditions were the same as in panel C except that that pups were administered intravitreally with 1 μg/0.5 μl/eye of scrambled, or p38β siRNA at P12, P13 and P15 and at P17 the retinas were isolated, stained with isolectin B4 and flat mounts were made and examined for filopodia formation. G. All the conditions were the same as in panel D except that the sections were stained for CD31, VEGFR3 and DAPI. H. All the conditions were the same as in panel F except that the flat mounts were examined for neovascularization. Retinal vascularization is shown in the first column. Neovascularization is highlighted in red in the second column. The third column shows the selected rectangular areas of the images shown in the first column under 10X magnification. I & J. Retinal neovascularization (I) and avascular areas (J) were determined as described in "Materials and Methods." The bar graphs represent quantitative analysis of 6 retinas. The values are presented as Mean ± SD. * $p < 0.01$ vs normoxia, normoxia + control siRNA; ** $p < 0.01$ vs hypoxia + control siRNA. Scale bar represents 50 μm and 20 μm in panel D, far left column and far right column, respectively, 20 μm in panels F & G and 300 μm and 50 μm in panel H, far left column and far right column, respectively.

Karkkainen, M.J., Petrova, T.V., 2000. Vascular endothelial growth factor receptors in the regulation of angiogenesis and lymphangiogenesis. Oncogene 19, 5598–5605.
Konisti, S., Kiriakidis, S., Paleolog, E.M., 2012. Hypoxia—a key regulator of angiogenesis and inflammation in rheumatoid arthritis. Nat. Rev. Rheumatol. 8, 153–162.
Kottakis, F., Polytarchou, C., Foltopoulou, P., Sanidas, I., Kampranis, S.C., Tsichlis, P.N., 2011. FGF-2 regulates cell proliferation, migration, and angiogenesis through an NDY1/KDM2B-miR-101-EZH2 pathway. Mol. Cell 43, 285–298.
Kuiper, E.J., Van Nieuwenhoven, F.A., de Smet, M.D., van Meurs, J.C., Tanck, M.W., Oliver, N., Klaassen, I., Van Noorden, C.J., Goldschmeding, R., Schlingemann, R.O., 2008. The angio-Fibrotic switch of VEGF and CTGF in proliferative diabetic retinopathy. PLoS One 3, e2675.
Lee, G.Y., Kenny, P.A., Lee, E.H., Bissell, M.J., 2007. Three-dimensional culture models of normal and malignant breast epithelial cells. Nat. Methods 4, 359–365.
Leonard, M.O., Howell, K., Madden, S.F., Costello, C.M., Higgins, D.G., Taylor, C.T., McLoughlin, P., 2008. Hypoxia selectively activates the CREB family of transcription factors in the in vivo lung. Am. J. Respir. Crit. Care Med. 178, 977–983.
Lobov, I.B., Cheung, E., Wudali, R., Cao, J., Halasz, G., Wei, Y., Economides, A., Lin, H.C., Papadopoulos, N., Yancopoulos, G.D., Wiegand, S.J., 2011. The Dll4/Notch pathway controls postangiogenic blood vessel remodeling and regression by modulating vasoconstriction and blood flow. Blood 117, 6728–6737.
Lobov, I.B., Renard, R.A., Papadopoulos, N., Gale, N.W., Thurston, G., Yancopoulos, G.D., Wiegand, S.J., 2007. Delta-like ligand 4 (Dll4) is induced by VEGF as a negative regulator of angiogenic sprouting. Proc. Natl. Acad. Sci. U. S. A. 104, 3219–3224.
Lux, A., Llacer, H., Heussen, F.M., Joussen, A.M., 2007. Non-responders to bevacizumab (Avastin) therapy of choroidal neovascular lesions. Br. J. Ophthalmol. 91, 1318–1322.
Mantamadiotis, T., Lemberger, T., Bleckmann, S.C., Kern, H., Kretz, O., Martin Villalba, A., Tronche, F., Kellendonk, C., Gau, D., Kapfhammer, J., Otto, C., Schmid, W., Schütz, G., 2002. Disruption of CREB function in brain leads to neurodegeneration. Nat. Genet. 31, 47–54.
Morishita, K., Johnson, D.E., Williams, L.T., 1995. A novel promoter for vascular endothelial growth factor receptor (flt-1) that confers endothelial-specific gene expression. J. Biol. Chem. 270, 27948–27953.
Nakatsu, M.N., Hughes, C.C., 2008. An optimized three-dimensional in vitro model for the analysis of angiogenesis. Methods Enzymol. 443, 65–82.
Nicoli, S., Knyphausen, C.P., Zhu, L.J., Lakshmanan, A., Lawson, N.D., 2012. miR-221 is required for endothelial tip cell behaviors during vascular development. Dev. Cell 22, 418–429.
Noguera-Troise, I., Daly, C., Papadopoulos, N.J., Coetzee, S., Boland, P., Gale, N.W., Lin, H.C., Yancopoulos, G.D., Thurston, G., 2006. Blockade of Dll4 inhibits tumour growth by promoting non-productive angiogenesis. Nature 444, 1032–1037.
Ober, E.A., Olofsson, B., Makinen, T., Jin, S.W., Shoji, W., Koh, G.Y., Alitalo, K., Stainier, D.Y., 2004. Vegfc is required for vascular development and endoderm morphogenesis in zebrafish. EMBO Rep. 5, 78–84.
Ohnuki, H., Jiang, K., Wang, D., Salvucci, O., Kwak, H., Sánchez-Martín, D., Maric, D., Tosato, G., 2014. Tumor-infiltrating myeloid cells activate Dll4/Notch/TGF-β signaling to drive malignant progression. Cancer Res. 74, 2038–2049.
Phng, L.K., Gerhardt, H., 2009. Angiogenesis: a team effort coordinated by Notch. Dev. Cell 16, 196–208.
Potula, H.S., Wang, D., Quyen, D.V., Singh, N.K., Kundumani-Sridharan, V., Karpurapu, M., Park, E.A., Glasgow, W.C., Rao, G.N., 2009. Src-dependent STAT-3-mediated expression of monocyte chemoattractant protein-1 is required for 15(S)-hydroxyeicosatetraenoic acid-induced vascular smooth muscle cell migration. J. Biol. Chem. 284, 31142–31155.
Ridgway, J., Zhang, G., Wu, Y., Stawicki, S., Liang, W.C., Chanthery, Y., Kowalski, J., Watts, R.J., Callahan, C., Kasman, I., Singh, M., Chien, M., Tan, C., Hongo, J.A., de Sauvage, F., Plowman, G., Yan, M., 2006. Inhibition of Dll4 signalling inhibits tumour growth by deregulating angiogenesis. Nature 444, 1083–1087.
Semenza, G.L., 2003. Targeting HIF-1 for cancer therapy. Nat. Rev. Cancer 3, 721–732.
Shaywitz, A.J., Greenberg, M.E., 1999. CREB: a stimulus-induced transcription factor activated by a diverse array of extracellular signals. Annu. Rev. Biochem. 68, 821–861.
Singh, N.K., Hansen III., D.E., Kundumani-Sridharan, V., Rao, G.N., 2013. Both Kdr and Flt1 play a vital role in hypoxia-induced Src-PLD1-PKCgamma-cPLA(2) activation and retinal neovascularization. Blood 121, 1911–1923.
Singh, N.K., Kotla, S., Dyukova, E., Traylor Jr., J.G., Orr, A.W., Chernoff, J., Marion, T.N., Rao, G.N., 2015. Disruption of p21-activated kinase 1 gene diminishes atherosclerosis in apolipoprotein E-deficient mice. Nat. Commun. 6, 7450.
Smith, L.E., Wesolowski, E., McLellan, A., Kostyk, S.K., D'Amato, R., Sullivan, R., D'Amore, P.A., 1994. Oxygen-induced retinopathy in the mouse. Investig. Ophthalmol. Vis. Sci. 35, 101–111.
Tammela, T., Zarkada, G., Nurmi, H., Jakobsson, L., Heinolainen, K., Tvorogov, D., Zheng, W., Franco, C.A., Murtomaki, A., Aranda, E., Miura, N., Ylä-Herttuala, S., Fruttiger, M., Mäkinen, T., Eichmann, A., Pollard, J.W., Gerhardt, H., Alitalo, K., 2011. VEGFR-3 controls tip to stalk conversion at vessel fusion sites by reinforcing Notch signalling. Nat. Cell Biol. 13, 1202–1213.
Tammela, T., Zarkada, G., Wallgard, E., Murtomaki, A., Suchting, S., Wirzenius, M., Waltari, M., Hellstrom, M., Schomber, T., Peltonen, R., Freitas, C., Duarte, A., Isoniemi, H., Laakkonen, P., Christofori, G., Ylä-Herttuala, S., Shibuya, M., Pytowski, B., Eichmann, A., Betsholtz, C., Alitalo, K., 2008. Blocking VEGFR-3 suppresses angiogenic sprouting and vascular network formation. Nature 454, 656–660.
Wang, Y., Nakayama, M., Pitulescu, M.E., Schmidt, T.S., Bochenek, M.L., Sakakibara, A., Adams, S., Davy, A., Deutsch, U., Luthi, U., Barberis, A., Benjamin, L.E., Mäkinen, T., Nobes, C.D., Adams, R.H., 2010. Ephrin-B2 controls VEGF-induced angiogenesis and lymphangiogenesis. Nature 465, 483–486.
Williams, C.K., Li, J.L., Murga, M., Harris, A.L., Tosato, G., 2006. Up-regulation of the Notch ligand delta-like 4 inhibits VEGF-induced endothelial cell function. Blood 107, 931–939.
Wu, D., Zhau, H.E., Huang, W.C., Iqbal, S., Habib, F.K., Sartor, O., Cvitanovic, L., Marshall, F.F., Xu, Z., Chung, L.W., 2007. cAMP-responsive element-binding protein regulates vascular endothelial growth factor expression: implication in human prostate cancer bone metastasis. Oncogene 26, 5070–5077.
Xing, J., Kornhauser, J.M., Xia, Z., Thiele, E.A., Greenberg, M.E., 1998. nerve growth factor activates extracellular signal-regulated kinase and p38 mitogen-activated protein kinase pathways to stimulate CREB serine 133 phosphorylation. Mol. Cell. Biol. 18, 1946–1955.
Zhao, D., Desai, S., Zeng, H., 2011. VEGF stimulates PKD-mediated CREB-dependent orphan nuclear receptor Nurr1 expression: role in VEGF-induced angiogenesis. Int. J. Cancer 128, 2602–2612.